MIT Joint Program on the Science and Policy of Global Change

Sensitivity of Climate to Diapycnal Diffusivity in the Ocean

Part I: ***Equilibrium State***. **Part II**: ***Global Warming Scenario***

Fabio Dalan, Peter H. Stone, Igor Kamenkovich and Jeffery Scott (Part I);
Fabio Dalan, Peter H. Stone and Andrei Sokolov (Part II)

Report No. 109
May 2004

The MIT Joint Program on the Science and Policy of Global Change is an organization for research, independent policy analysis, and public education in global environmental change. It seeks to provide leadership in understanding scientific, economic, and ecological aspects of this difficult issue, and combining them into policy assessments that serve the needs of ongoing national and international discussions. To this end, the Program brings together an interdisciplinary group from two established research centers at MIT: the Center for Global Change Science (CGCS) and the Center for Energy and Environmental Policy Research (CEEPR). These two centers bridge many key areas of the needed intellectual work, and additional essential areas are covered by other MIT departments, by collaboration with the Ecosystems Center of the Marine Biology Laboratory (MBL) at Woods Hole, and by short- and long-term visitors to the Program. The Program involves sponsorship and active participation by industry, government, and non-profit organizations.

To inform processes of policy development and implementation, climate change research needs to focus on improving the prediction of those variables that are most relevant to economic, social, and environmental effects. In turn, the greenhouse gas and atmospheric aerosol assumptions underlying climate analysis need to be related to the economic, technological, and political forces that drive emissions, and to the results of international agreements and mitigation. Further, assessments of possible societal and ecosystem impacts, and analysis of mitigation strategies, need to be based on realistic evaluation of the uncertainties of climate science.

This report is one of a series intended to communicate research results and improve public understanding of climate issues, thereby contributing to informed debate about the climate issue, the uncertainties, and the economic and social implications of policy alternatives. Titles in the Report Series to date are listed on the inside back cover.

Henry D. Jacoby and Ronald G. Prinn,
Program Co-Directors

For more information, please contact the Joint Program Office

Postal Address: Joint Program on the Science and Policy of Global Change
77 Massachusetts Avenue
MIT E40-428
Cambridge MA 02139-4307 (USA)

Location: One Amherst Street, Cambridge
Building E40, Room 428
Massachusetts Institute of Technology

Access: Phone: (617) 253-7492
Fax: (617) 253-9845
E-mail: globalchange@mit.edu
Web site: http://MIT.EDU/globalchange/

Sensitivity of Climate to Diapycnal Diffusivity in the Ocean
Part I: *Equilibrium State*

Fabio Dalan[*], Peter H. Stone[†], Igor Kamenkovich[‡] and Jeffery Scott[†]

Abstract

The diapycnal diffusivity in the ocean is one of the least known parameters in current climate models. Measurements of this diffusivity are sparse and insufficient for compiling a global map. Inferences from inverse methods and energy budget calculations suggest as much as a factor of 5 difference in the global mean value of the diapycnal diffusivity. Yet, the climate is extremely sensitive to the diapycnal diffusivity. In this paper we study the sensitivity of the current climate to the diapycnal diffusivity using a coupled model with a 3-dimensional global ocean component with idealized geometry. In a subsequent paper we analyze the sensitivity of the climate change to the same parameter.

Our results show that, at equilibrium, the strength of the thermohaline circulation in the North Atlantic scales with the 0.44 power of the diapycnal diffusivity, in contrast to the theoretical value of 2/3. On the other hand, the strength of the circulation in the South Pacific scales with the 0.63 power of the diapycnal diffusivity. The implication is that the amount of water upwelling from the deep ocean may be regulated by the diapycnal diffusion in the Indo-Pacific Ocean.

The vertical heat balance in the ocean is controlled by: in the downward direction, (i) advection and (ii) diapycnal diffusion; in the upward direction, (iii) isopycnal diffusion and (iv) bolus velocity (GM) advection. The size of the latter three fluxes increases with diapycnal diffusivity, because the thickness of the thermocline also increases with diapycnal diffusivity leading to greater isopycnal slopes at high latitudes, and hence enhanced isopycnal diffusion and GM advection. Thus larger diapycnal diffusion is compensated for by changes in isopycnal diffusion and GM advection. Little change is found for the advective flux because of compensation between downward and upward advection.

We present sensitivity results for the hysteresis curve of the thermohaline circulation. The stability of the climate system to slow freshwater perturbations is reduced as a consequence of a smaller diapycnal diffusivity. This result confirms the findings of 2-dimensional climate models. However, contrary to the results of these studies, a common threshold for the shutdown of the thermohaline circulation is not found in our model.

Contents

[*NOTE*: Part II: *Global Warming Scenarios* begins on page 27]

[*] Corresponding author. Postal address: Via Cavour 44/e, 35030 Rubano (PD), Italy. Tel: +39 049 328 47 80 663. Email: fabio.dalan@alum.mit.edu

[†] Joint Program on the Science and the Policy of Climate Change, MIT, Cambridge, Massachusetts, USA

[‡] Joint Institute for the Study of the Atmosphere and the Oceans, University of Washington, Seattle, USA

1. INTRODUCTION

In numerical simulations, the equilibrium state of the global ocean circulation is very sensitive to the value and the location of the diapycnal diffusivity (*e.g.*, Bryan, 1987; Cummins *et al*., 1990; Scott and Marotzke, 2002). Yet, a global map of the diapycnal diffusivity, based on observations, is not available. Measurements are sparse in space and time, ranging from 5 cm^2/s above the mid-ocean ridge, to 0.1 cm^2/s over smooth topography (Polzin *et al*., 1997) and in the thermocline (Ledwell *et al*., 2000). Inference from the density structure of the global ocean suggests that the global average diapycnal diffusivity is of the order of 1 cm^2/s (Munk, 1966; Munk and Wunsch, 1998) while estimations of energy dissipation across the ocean give a global value closer to 0.2 cm^2/s (Huang, 1999). Still, ocean general circulation models (GCMs) use values for the diapycnal diffusivity ranging over an interval larger than the one given from measurements and calculations[1]. Several properties of the climate system are potentially affected by the diapycnal diffusivity. We focus our attention on the scaling behavior of the thermohaline circulation (THC) and the ocean heat transport, the vertical heat balance in the ocean and the stability of the climate under a quasi-static freshwater perturbation.

The sensitivity of the present ocean circulation to the diapycnal diffusivity has been previously studied in ocean GCMs. The THC is more sensitive to the diapycnal diffusivity in the tropics and along the eastern and western boundaries (Scott and Marotzke, 2002), while in the vertical direction the sensitivity is high at the bottom of the thermocline (Cummins *et al*., 1990). These results have been confirmed also for a global ocean GCM (OGCM) coupled to an energy balance model (Bugnion and Hill, 2004a,b,c). Scott (2000) showed that the strength of the thermohaline circulation does not change considerably whether mixing is localized along the lateral boundaries or it is uniformly distributed over the ocean, as long as the area integrated diffusivity is the same in both cases. For the sake of simplicity, in the present study the diapycnal diffusivity is uniform across and within the ocean basins.

The sensitivity of the THC strength to the diapycnal diffusivity has been examined in single-hemisphere OGCMs with idealized topography (Bryan, 1987; Marotzke, 1997; Park and Bryan, 2000; Scott, 2000). A simple scaling argument, based on the application of advective-diffusive balance and thermal wind (Welander, 1971) is in close agreement with the results from these simple models. Marotzke (1999) and Marotzke and Klinger (2001) present theories for predicting the overturning strength in a single hemisphere and (closed) single basin, respectively. Gnanadesikan (1999) derives a cubic equation which relates pycnocline depth (and hence overturning strength) which includes the effect of wind forcing and diapycnal mixing for a single basin configuration with a southern channel. However, the scaling behavior of the overturning circulation in a multi-basin configuration is largely untested and its dynamics poorly understood;

[1] According to CMIP2 (Coupled Model Intercomparison Project (http://www-pcmdi.llnl.gov/cmip/cmiphome.html) documentation, for example, the Australian model from the Bureau of Meteorology Research Center assumes a constant diapycnal diffusivity of 20 cm^2/s.

here, we show scaling results using our global, coupled configuration, discussing our results in the context of the simple idealized OGCM studies. We also diagnose heat transport in our global model, again comparing our results with those of the documented idealized OGCM studies.

The analysis of the vertical heat balance in the ocean is a very useful tool for understanding ocean heat uptake and therefore ocean dynamics and thermodynamics. The sensitivity of such balance at equilibrium indicates whether the relative magnitude of the processes transporting heat vertically depends on the diapycnal diffusion. A forthcoming paper (Dalan *et al*., 2004) will address the question of whether the heat uptake in global warming experiments depends on the diapycnal diffusion.

Gregory (2000) analyzed the heat balance of the vertical fluxes both at equilibrium and in a global warming experiment. He combined together the advective fluxes (Eulerian and parameterized eddy advection) and the diffusive fluxes (isopycnal and diapycnal) when analyzing the global ocean balance. While, investigating the balance for different latitude bands and basins, he limited the analysis to a single depth level (160 m). The heat balance at every depth level is presented by Huang *et al*. (2003). However, he also lumped together the isopycnal diffusive flux and the bolus velocity (hereinafter GM) advective flux.

The ocean's possible equilibrium states are explored in hysteresis experiments where the freshwater flux in the Atlantic Ocean increases (decreases) until the shutdown (recovery) of the THC is reached. The magnitude of freshwater flux increment is made small enough so that the state of the model is always near the equilibrium. Hysteresis experiments tell us how far the equilibrium climate of a model is from the collapse of the THC due to enhanced freshwater flux in the North Atlantic.

Ganopolsky *et al*. (2001) and Schmittner and Weaver (2001) suggested that the stability of the climate system is reduced for a reduction in vertical diffusivity, *i.e*., the collapse of the circulation is achieved at a smaller freshwater perturbation for small values of the vertical diffusivity. Schmittner and Weaver (2001) noticed also that a common threshold of a minimum THC strength seems to exist, below which the circulation collapses. These results may be biased by the use of models with 2D ocean basins. Such models differ substantially from a 3D ocean model in several aspects, among which are the need to parameterize the effect of rotation and the neglect of zonal variations in the North Atlantic. In 2D ocean models, important processes like convection and downward advection occur at the same location, while, in 3D ocean models with idealized topography, they can occur at opposite sides of the Atlantic basin (Marotzke and Scott, 1999). Recently, a study with a 3D OGCM (Prange *et al*., 2003, their fig. 6) with linearized dynamics confirmed the early collapse of the THC with decreasing vertical mixing but no common threshold was observed.

In analyzing the sensitivity of the current climate to changes in diapycnal diffusivity, we will investigate the power-law relation of the THC and the ocean heat transport in the context of a coupled model with a 3D global ocean component. We perform an analysis of the vertical heat

balance for the current climate, dividing the heat fluxes into *all* its components, and we study the sensitivity of the vertical heat balance at every depth to changes in diapycnal diffusivity. Lastly, we perform a sensitivity study of the hysteresis curve to diapycnal diffusivity, using a coupled model that includes a 3D ocean component and the full non-linear momentum equations.

The paper is organized as follows. In Section 2 we describe the numerical model. Section 3 contains the analysis of the equilibrium ocean circulation: here, the scaling behavior of the THC strength and the ocean heat transport is presented; Section 4 illustrates the sensitivity of the vertical heat balance in the ocean to the diapycnal diffusivity and in Section 5 the same sensitivity is presented for the hysteresis cycle of the THC. Finally, Section 6 contains the conclusions.

2. MIT EARTH MODEL OF INTERMEDIATE COMPLEXITY

More details about the model can be found in Kamenkovich *et al*. (2000, 2002).

2a. Atmospheric Component

The 2-dimensional zonally averaged statistical-dynamical atmospheric model was developed by Sokolov and Stone (1998) on the basis of the GISS GCM (Hansen *et al*., 1983). The model solves the zonally averaged primitive equations in latitude-pressure coordinates. The grid of the model consists of 24 points in the meridional direction, corresponding to a resolution of 7.826°, and 9 layers in the vertical. In addition to the parameterizations used in the GCM, the model includes the parameterization of heat, moisture and momentum transports by large scale eddies (Stone and Yao, 1990). It has a complete moisture and momentum cycle.

Most of the physics and parameterizations of the atmospheric model derive from the GISS GCM. The 2D model, as well as the GISS GCM, allows four different types of surfaces in the same grid cell, namely: open ocean, sea-ice, land, and land-ice. The surface characteristics, as well as turbulent and radiative fluxes, are calculated separately for each kind of surface, while the atmosphere above is assumed to be well-mixed zonally. The atmospheric model uses a realistic land/ocean ratio for each latitude band. More detailed description of the model can be found in Sokolov and Stone (1998) and Prinn *et al*. (1999).

2b. Ocean Component

The ocean component of the coupled model is the MOM2 model (Pacanowski, 1996) with idealized geometry (**Figure 1**). It consists of two rectangular “pool” basins connected by a Drake Passage that extends from 64°S to 52°S. The Indo-Pacific (hereinafter Pacific) pool extends from 48°S to 60°N and is 120° wide while the Atlantic pool extends from 48°S to 72°N and is 60° wide.

The meridional resolution is 4° and the zonal resolution varies from 1° near the boundaries to 3.75° in the interior of the ocean. Better resolution of the boundary currents has been shown to improve the meridional heat transport in an ocean GCM (Kamenkovich *et al*., 2000). In the vertical, the model has 15 layers of increasing thickness from 53 m at the surface to 547 m at depth. The bottom of the ocean is flat and 4500 m deep everywhere except in the Drake Passage where there is a sill 2900 m deep.

No-slip boundary conditions are applied to the lateral walls and free-slip boundary conditions at the bottom of the ocean, except in the Antarctic Circumpolar Current (ACC) where bottom drag is applied. Boundary conditions for tracers are insulating at lateral walls and bottom of the ocean. The Gent McWilliams parameterization scheme, in its "bolus" form, is used to account for the small-scale eddy induced transport (Gent and McWilliams ,1990). Mixing caused by small-scale process occurs along and across isopycnals. Hence, the mixing tensor is rotated to be aligned with the isopycnal slope (Redi, 1982). No background horizontal diffusivity is used. **Table 1** summarizes the mixing parameters of the ocean model in its standard configuration.

Table 1. Sub-grid scale parameters of the ocean model in standard configuration.

Parameter	Value	Units
Isopycnal Diffusivity	1000	m^2/s
Diapycnal Diffusivity	0.5	cm^2/s
Thickness Diffusivity	1000	m^2/s
Lateral Viscosity	50000	m^2/s
Vertical Viscosity	100	cm^2/s

2c. Coupling, Spinup and Experimental Setup

Coupling takes place twice a day. The atmospheric model calculates 12-hour mean values of heat and freshwater fluxes over the open ocean (Ho, Fo), their derivatives with respect to the sea surface temperature, SST, (dHo/dSST, dFo/dSST) and the wind stress. These quantities are then used to calculate the longitudinal variations of the heat and freshwater fluxes for the ocean model. Thus:

$$Ht = Ho + (dHo/dSST)(SST - SST^*), \quad (1)$$

$$Fw = Fo + (dFo/dSST)(SST - SST^*). \quad (2)$$

SST* denotes the zonal average SST and thus the last term on the right-hand-side allows for the zonal variations of the fluxes as well as the zonal transfer of heat and moisture among ocean basins. The last term in Eq. 2 represents variations in evaporation only, *i.e*., there are no longitudinal variations in precipitation in our model. The wind stress is independent of longitude. The atmosphere and ocean models are coupled through their anomalous fluxes of heat and freshwater. From Eqs. 1 and 2 the fluxes of heat (Ho) and freshwater (Fo) are:

$$Ho(x,y) - Ho^{spin}(x,y) = Ha(y) - Ha^{spin}(y),$$

$$Fo(x,y) - Fo^{spin}(x,y) = Fa(y) - Fa^{spin}(y),$$

where Ho^{spin} and Fo^{spin} are the fluxes diagnosed after the spinup of the ocean-only model and Ha^{spin} and Fa^{spin} are the fluxes calculated from spinup of the atmospheric model alone. A similar procedure is used for the wind stress.

The ocean is integrated for 12 hours forced by the above fluxes and provides to the atmosphere the zonal mean SST. Asynchronous integration (Bryan, 1984) is used, with 12 hour

time-step for the tracer equations and 1 hour time-step for the momentum equations. This is sufficient to resolve the annual cycle (Kamenkovich *et al*., 2002). The coupled model takes about 4 hours to complete a hundred years integration in a 2.2 GHz Dell workstation with 2 GB memory. For more details about the coupling procedure refer to Kamenkovich *et al*. (2002).

After separate spinup of the atmospheric and oceanic components they are coupled and spun up for an additional 1000 years for each value of the diapycnal diffusivity: 0.1, 0.2, 0.5 and 1.0 cm^2/s. The model was considered to be at equilibrium when the global average heat flux entering the ocean fluctuates around the zero value. Peak-to-peak fluctuations of SAT are confined to two tenths of a degree and represent the natural variability of the climate as simulated by this model, comparable with that found in more sophisticated GCMs (Houghton *et al*., 2001, their fig. 12.1). The natural variability (estimated by the peak-to-peak variations) of the THC goes from few tenths of Sverdrups for small diapycnal diffusivity, up to 2 Sv for large diapycnal diffusivity, while in full 3D coupled GCMs the same quantity is of the order of 2 to 4 Sv (Houghton *et al*., 2001, fig. 9.21).

3. SCALING BEHAVIOR OF THE OCEAN CIRCULATION

3a. Thermohaline Circulation

As vertical diffusivity k_v increases, the thermocline deepens and the THC strength increases, as shown in **Figure 2** for the Atlantic Ocean. In the mid-and high-latitude Northern Pacific, there is little change in meridional overturning, as there is only weak circulation in this region in either the large or small k_v runs (**Figure 3**). However, as shown in this latter figure, there is considerable increase in upwelling in the tropical and sub-tropical Pacific for larger k_v.

Using idealized geometry, single-hemisphere (rapidly restored) ocean models, it has been shown robustly that the scaling of overturning follows an approximate 2/3rds power law (Bryan, 1987; Colin de Verdiere, 1988; Park and Bryan, 2000; Scott, 2000). This power law is supported by a simple scaling relationship (Welander, 1971) and a more complicated theory for the overturning circulation (Marotzke, 1997), both of which are grounded in the thermal wind relationship. Here, our coupled model is considerably more complicated: we have a more complicated "boundary condition" at the ocean surface, we include wind forcing, and perhaps most significantly, we have a global configuration (*i.e*., a multi-basin inter-hemispheric circulation connected by a circumpolar channel). Nevertheless, we present a scaling analysis in the spirit of the canonical single-hemisphere results, as shown in **Figure 4** for the North Atlantic maximum and **Figure 5** for the South Pacific maximum (observed roughly at 32°S).

In both cases, an approximate straight-line fit is observed. In the North Atlantic, the overturning maximum scales as the 0.44 power (as measured by a best-fit line), whereas in the South Pacific the maximum scales as the 0.63 power. We are aware of only two studies which examine the scaling of meridional overturning in a global model, Wright and Stocker (1992) and Knutti *et al*. (2000), both using a simplified ocean model consisting of interconnected zonally-

averaged ocean basins. Wright and Stocker's results (best-fit scaling laws of 0.46 and 0.68 for the Atlantic and Pacific, respectively) are close to ours, despite their use of a relaxation boundary conditions for temperature and salinity. Knutti *et al*. (2000) obtains roughly the same result for the North Atlantic maximum, again using restoring boundary conditions. This later study uses the Gent-McWilliams parameterization for mesoscale eddies, as does our model.

We now address the differences between our model and those used in past studies, and how these differences might affect the observed scaling behavior.

(Local) Wind Forcing. Local wind forcing does affect the depth of the zonally-averaged thermocline, which presumably has some effect on the meridional overturning circulation (by local, we mean intra-hemispheric wind forcing; we will address wind forcing over the southern channel below). However, past studies which examine the single-hemisphere scaling with and without wind forcing suggest only a modest wind effect (Zhang *et al*., 1999; Vallis, 2000), most noticeable at low diffusivities (*i.e*., the overturning does not drop off as dramatically if wind forcing is present). Thus, local winds might boost the maximum overturning slightly for our weak kappa runs, particularly our 0.1 and 0.2 cm^2/s experiments, but we would not expect it to preclude us from obtaining a scaling relationship similar to that of the simple models.

Atmospheric Coupling. In the canonical model results, temperature (and/or density) is either prescribed or rapidly restored at the surface. Here, we have a flux condition for freshwater forcing. Our effective boundary condition for temperature (*i.e*., from the coupled atmosphere) is a hybrid flux-relaxation boundary condition: although the loss of heat at the ocean surface is closer in spirit to a flux boundary condition, we do use a "flux adjustment" and thus our runs effectively include a strong relaxation component. We also show the scaling of maximum overturning in the North Atlantic with k_v for the uncoupled model; not surprisingly, there is only a slight change in the best-fit power law.

Thus, we conclude that the most significant novelty with respect to the surface boundary conditions is our use of a freshwater flux (note this flux is little changed between the different k_v runs). Zhang (1998) and Zhang *et al*. (1999) are the only studies that we are aware of that examine the scaling argument given mixed boundary conditions, albeit in a idealized single hemisphere configuration. Using salinity conservation in a single hemisphere, these authors show that when haline forcing dominates, a 1/2 power law emerges, whereas a 2/3 law is recovered for dominant temperature forcing. Zhang (1998) found an approximate 1/2 power law for flux conditions in temperature and salinity, but did not show a comparable scaling for mixed boundary conditions. Although it is not clear to what extent, if any, the analytical scaling of Zhang *et al*. (1999) applies to our configuration, it is interesting that we too achieve an approximate 1/2 power law in the North Atlantic-where salinity forcing is thought to play a large role in determining the rate of sinking. In the South Pacific, however, our observed scaling law is closer to that predicted by Zhang's temperature-dominated extreme.

Global Configuration. While the role of mixing is straightforward in the idealized single-hemisphere configuration, there is considerable debate as to the importance of mixing in the global configuration. Specifically, Toggweiler and Samuels (1993) argue that wind forcing over the ACC effectively controls the rate of sinking in the North Atlantic. Gnanadesikan (1999) presents a simple theory for overturning in a single ocean basin with a circumpolar channel, effectively combining the effect of wind forcing (in the channel) and diapycnal mixing; the scaling here has been verified in other models studies (Klinger *et al*., 2003). Unfortunately, Gnanadesikan's model produces a cubic equation governing pycnocline depth, and therefore would not predict a simple power-law scaling. Moreover, in this theory, all mixing-induced upwelling occurs in the tropics of the single basin, whereas our model is a multi-basin configuration. In fact, it seems reasonable to assume that most of the mixing-induced upwelling occurs in the Pacific Basin, given the greater area. (In idealized single hemisphere studies, Samelson (1999) and Scott and Marotzke (2002) argue that it is the area-integrated mixing that is the critical quantity in terms of supporting a vigorous overturning). The work of Bugnion and Hill (2004b,c) supports this idea: the adjoint sensitivity of the THC strength to the diapycnal diffusion is large in the tropical regions of all ocean basins.

Hence, we argue that although the sinking in the Northern Atlantic is the traditional focus of climate research, the scaling of the South Pacific cell is the closer comparison to the canonical single-hemisphere studies. This conjecture is supported by the near agreement of our power law fit with the classical 2/3 power law (Fig. 5). The scaling of the North Atlantic is more problematic. It is not clear what the y-intercept in Fig. 4 should be, but it does seem to imply a significant residual Circulation in the "no-mixing" limit. Further exploration of THC scaling in a global configuration is left for future studies.

3b. Heat Transport

In the Northern Hemisphere, the power-dependence between global ocean heat transport and diapycnal diffusivity is 0.24 (**Figure 6**). At the location of the maximum transport (from 18°N for diffusivity 0.1 cm^2/s to 26°N for diffusivity 1.0 cm^2/s), the strength of the meridional streamfunction for the global ocean depends on the 0.37 power of the diapycnal diffusivity (**Table 2**). At the same location, the temperature difference between the poleward and equatorward branches of the North Atlantic overturning cell goes from 26°C, for diffusivity 0.1 cm^2/s, to 20°C, for diffusivity 1.0 cm^2/s, having a –0.12 power-dependence on the diapycnal diffusivity (Table 2). The product of overturning strength and the temperature difference between the poleward and equatorward branches of the North Atlantic overturning cell explains the relation between the maximum heat transport and the diapycnal diffusivity (Fig. 6). In our model, in fact, the main component of the poleward heat transport is given by the thermohaline circulation. Both in spinup and coupling procedure the SST is restored to its zonal average (Eq. 1), hence the heat transport by the gyre circulation is greatly reduced. The absence of heat

Table 2. Sensitivity of heat transport to the diapycnal diffusivity: Maximum heat transport (A), maximum streamfunction (B) and temperature difference between the poleward and equatorward branches of the North Atlantic overturning cell (C) for the global ocean. Both B and C are calculated at the location of maximum global ocean heat transport.

	Diapycnal Diffusivity	**cm^2/s**	**0.1**	**0.2**	**0.5**	**1.0**
A	Maximum heat transport	PW	0.72	0.84	1.08	1.25
B	Maximum streamfunction at A	Sv	11.4	12.8	19.8	26.0
C	THC vertical temperature difference at A	°C	26.2	25.1	22.1	20.3

transport by the gyre circulation explains why the North Pacific contribution to the global heat transport in the Northern Hemisphere is negligible (**Figure 7c**).

In the Southern Hemisphere, the dependence of the poleward heat transport to the diapycnal diffusion goes with the power of 0.45 for the global ocean and 0.35 for the Pacific component (not shown). Although the Pacific Ocean contributes the most to the global heat transport in the Southern Hemisphere, the Southern Atlantic contribution cannot be ignored (Figure 7b and c). The latter is relatively insensitive to the diapycnal diffusivity explaining the decrease of power from the global ocean heat transport to the Pacific component in the Southern Hemisphere. The insensitivity of the Southern Atlantic heat transport to diapycnal diffusion may be relevant for the behavior of the THC. The strength of the THC is correlated with the steric height difference between the Northern and Southern Atlantic (Hughes and Weaver, 1994; Thorpe *et al*., 2001), which in turn is related to the integrated density over a water column. At each latitude band, the heat transport, or better its divergence, affects the density of the water column thus the THC strength. This version of the MIT-EMIC has idealized geometry; in particular the African continent extends to 48°S rather than a more realistic 30°S. Moreover, processes like brine rejection, responsible for the formation of the Antarctic Bottom Water, are not modeled. Hence the insensitivity of the Southern Atlantic heat transport to the diapycnal diffusivity may be biased in our model. Further investigation with a realistic geometry coupled GCM is needed.

In general we find a smaller power-law dependence between oceanic heat transport and diapycnal diffusivity compared to previous studies with OGCMs. Our findings do not agree with the scaling argument either in the Northern Hemisphere or in the Southern Hemisphere. The scaling argument may need to be revised to include feedbacks between the ocean and the atmosphere and the effect of realistic Southern Ocean geometry. In addition, as seen above, the temperature difference between the poleward and equatorward branches of the North Atlantic overturning cell affects the power-law for the Northern Hemisphere heat transport. The temperature difference sensibly depends on the temperature of the water sinking in the North Atlantic which depends, among other things, on the ocean overturning circulation and both the atmospheric and oceanic meridional heat transports. The scaling argument, by its construction, cannot capture the relation between the above mentioned temperature difference, the strength of the overturning and the meridional heat transports.

4. VERTICAL HEAT BALANCE

4a. Control Experiment

The vertical heat balance of the global ocean consists of downward diapycnal diffusion and eulerian advection (hereinafter advection) balancing upward fluxes by isopycnal diffusion and bolus velocity (hereinafter GM) advection (**Figure 8a**). Convection plays a negligible role in all runs, the reason being explained in the appendix. Following Gregory (2000), we divide the global ocean in three latitude bands: the Southern Ocean, southward of 30°S, the tropics, between 30°S and 30°N and the Northern Ocean, northward of 30°N.

Diapycnal diffusion, the major contributor to the downward heat flux for the global ocean (Fig. 8a), is concentrated in the tropical region although considerable diapycnal flux also occurs at high latitudes (Fig. 8b, c and d). However, while the tropical diapycnal flux is due to the presence of strong vertical temperature gradients, in high latitudes the diapycnal flux arises to partially compensate for the stronger and opposite isopycnal flux (Fig. 8b and d). Eulerian advection takes heat downward at high latitudes but mostly in the Northern Ocean (Fig. 8b and d) and upward in the tropics (Fig. 8c) so that the global contribution of the advective flux is the smallest among all the components[2] (Fig. 8a). Additionally, GM advection and isopycnal diffusion dominate at high latitudes, where the isopycnal slope is elevated (Fig. 8b and d). The Northern Ocean fluxes are representative of the North Atlantic region, where most of the dynamics in this model takes place, while fluxes in the tropical Pacific are about twice as large as the tropical Atlantic ones, because the area extent of the former is twice the area of the latter (not shown).

Figure 8 does not include the surface heat flux, presented in **Figure 9**. Heat is entering in the tropical region at a rate of 13 Wm^{-2} (16 Wm^{-2} Atlantic and 11 Wm^{-2} Pacific) and leaving the ocean at high latitudes at a rate of –13 Wm^{-2} in the Southern Ocean and –23 Wm^{-2} in the Northern Ocean (–53 Wm^{-2} Atlantic and –4 Wm^{-2} Pacific).

Locally, downwelling occurs in the east side of the North Atlantic basin. The deep water formed in this region flows westward and southward for upwelling in the western side of the basin, as well as in the Southern Ocean and in the interior of the basins (**Figure 10a**). Downward advection steepens the isopycnals generating elevated GM velocities. Hence, strong eulerian advective fluxes are contrasted by equally strong and opposite GM fluxes throughout the oceans (Fig. 10b). At high latitudes, diapycnal diffusion tends to compensate isopycnal diffusion (Fig. 10c and d).

Gregory (2000) performed an analysis of the heat balance at 160 m depth for the HadCM2 climate model combining together diffusive fluxes (isopycnal and diapycnal) while the advective fluxes are eulerian only since no GM scheme is employed. The author finds that, for the global ocean, total downward heat advection is balanced by upward diffusion, opposite to the balance assumed in one-dimensional upwelling-diffusion models. In HadCM2, Southern Ocean fluxes

[2] Excluding convection.

dominate the global budget, thanks to a strong Deacon cell (47 Sv) that extends from 35°S to 65°S. Heat is taken down at 35°S by advection and it is lost along the way by isopycnal diffusion. Water then upwells in much colder sites around 65°S. In the MIT-EMIC the Deacon cell is significantly weaker (18 Sv) and its extension is limited between 48°S and 64°S. Although the vertical heat balance at different latitude bands in our model agrees with Gregory's (2000) picture (downward advection balances upward diffusion at high latitudes and the opposite in the tropics), the global budget for the MIT-EMIC is dominated by the tropical region, thus opposite to Gregory (2000) and in agreement with one-dimensional upwelling-diffusive models.

4b. Sensitivity to Diapycnal Diffusion

Four control experiments have been carried out, with the same model being spun up with different values of the diapycnal diffusivity, namely: 0.1, 0.2, 0.5 and 1.0 cm^2/s. Although the current estimates for the global average diapycnal diffusivity are 0.2 cm^2/s (Huang, 1999) and 1.0 cm^2/s (Munk and Wunsch, 1998), we compare in detail the differences between the control runs with diapycnal diffusivity 0.1 cm^2/s and 0.5 cm^2/s, referring to the former case as the "small diffusivity model" and to the latter as the "standard diffusivity model." The conclusions drawn for the small diffusivity model can be applied to the simulations using diapycnal diffusivity 0.2 cm^2/s while the standard diffusivity case is similar, in its behavior, to the simulation with diapycnal diffusivity 1.0 cm^2/s. The reason behind the choice for diapycnal diffusivity 0.1 to 0.5 cm^2/s instead of 0.2 to 1.0 cm^2/s is that the former doublet gives a more representative range of where the strength of the THC in the real ocean may be found. The strength of the THC for the experiments with diapycnal diffusivity 0.1 and 0.5 cm^2/s is 12 and 26 Sv respectively while the latest estimates for the same quantity is 15 Sv (Ganachaud and Wunsch, 2003).

In the experiments with small diffusivity, there remains a very small net flux into the ocean, even after very long integration times (12,000 years in the case of diffusivity 0.1). Nevertheless the qualitative result is clear. The vertical heat balance for the small diffusivity model is not much different from the standard diffusivity model. Isopycnal diffusion and GM advection dominate the removal of heat from the deep ocean at high latitudes while advection in the Northern Ocean is a major heat source for the deep ocean. The major difference between the two simulations is in the tropical region. The diapycnal flux is significantly reduced in the small diffusivity model, as expected, and it is no longer the major heat source for the deep ocean, as it is for the standard diffusivity model (not shown). Moreover, the advective flux, upward in the tropical region, is sensibly reduced, hence the total advective flux, downward for the global ocean, slightly increases for the small diffusivity model. In fact, the strength of the THC strongly decreases with decreasing diapycnal diffusivity (Fig. 2) but compensation between decrease in downward warming at high latitudes and decrease in upward cooling in the tropics leads to a small increase in the global advective flux. As for the standard diffusivity model, in the small diffusivity model the tropical region is dominated by the Pacific basin while the Northern Ocean is dominated by the Atlantic basin.

The magnitude of all fluxes is reduced with smaller diapycnal diffusivity (**Figure 11**) as expected from adjoint sensitivity studies (Huang *et al*., 2003, their figs. 5 and 11). Total advection always balances total diffusion since convection is always negligible in this version of the MIT-EMIC. Fluxes at the bottom of the first layer are 0.7 Wm^{-2} in the small diffusivity model (Fig. 11a) and one order of magnitude larger for the standard diffusivity model (Fig. 11c), rapidly decreasing with depth. Reduced diapycnal diffusion leads to smaller diapycnal fluxes and shallower thermocline at tropical latitudes. As a consequence, the isopycnal slopes at high latitudes are reduced and so are the vertical isopycnal and GM fluxes. However, in the small diffusivity case, the tropics are no longer the dominant region at all depths, as it is for the standard diffusivity model, and in the upper 800 m of ocean and the advective-diffusive balance is reversed (Fig. 11a and c).

5. QUASI-STATIC FRESHWATER PERTURBATION

Sensitivity experiments of the hysteresis curve to the diapycnal diffusivity are performed with the MIT-EMIC. The result is depicted in **Figure 12**. Note that, in the hysteresis experiments, the freshwater input is not balanced by any freshwater export in other regions of the oceans, therefore the global salinity is not conserved. As in previous sensitivity studies of the hysteresis curve (Ganopolsky *et al*., 2001; Schmittner and Weaver, 2001; Prange *et al*., 2003), the circulation is more unstable for a smaller value of the diapycnal diffusivity. In order to induce the THC to collapse, a freshwater input of 0.52 Sv is needed with diapycnal diffusivity of 0.5 cm^2/s while 0.37 Sv are needed with 0.2 cm^2/s diapycnal diffusivity. The main reason for the early collapse in low vertical diffusion models is most likely related to their smaller overturning in the equilibrium state. The equilibrium overturning strength for the current climate is proportional to the diapycnal diffusivity (Bryan, 1987) therefore also the salt transport into high latitudes. The latter helps sustain the thermohaline circulation, hence, the system is more unstable to freshwater perturbations for weaker equilibrium meridional circulation.

The THC collapses around 10 Sv in the standard diffusivity model (0.5 cm^2/s) and around 6 Sv in the low diffusivity model (0.2 cm^2/s). Thus, a common threshold for the collapse does not exist in this particular model as in the 3D OGCM of Prange *et al*. (2003). In 2.5D models, threshold for the collapse of the THC is relatively insensitive to the diapycnal diffusivity, suggesting that the over-simplified dynamics of 2D models affects the stability characteristic of the THC.

For smaller values of the diapycnal diffusivity, a smaller amount of freshwater forcing is needed to allow the recovery of the THC. The thermohaline circulation resumes when the freshwater forcing in the North Atlantic is about 0.34 Sv for diapycnal diffusivity 0.5 cm^2/s and 0.23 Sv for diapycnal diffusivity 0.2 cm^2/s. This is in agreement with the behavior of 2.5D models but in contrast with the 3D model behavior of Prange *et al*. (2003). When the THC is in the “shutdown” mode, the previous authors notice that the gyre transport gives an important contribution to the salt balance at the surface in the North Atlantic. Thus, differences in gyre

transport can be used to explain the different freshwater threshold for the recovery of the THC. This argument can be employed also to explain the differences between our model and the Prange *et al*. (2003) model. In the coupling procedure between the 2D atmosphere and the 3D ocean (Section 2c), both heat and freshwater fluxes are relaxed towards the global zonal mean as an attempt to capture the zonal variations of the fluxes (Eqs. 1 and 2). The consequence is a reduced gyre transport, as confirmed by the small northward heat transport in the North Pacific (Fig. 7c). The Prange *et al*. (2003) model employs linear momentum equations and it lacks feedback between the ocean and the atmosphere, two important differences from the MIT-EMIC. It is not clear how these differences would affect the hysteresis curve although the former model is clearly sensitive to the formulation of the surface boundary conditions (Prange *et al*., 2003, their fig. A4).

For both values of the diapycnal diffusivity, the strength of the THC in the recovery process overshoots the value obtained when increasing freshwater flux. This is indicative of a fast rate of decrease in the forcing. Two additional experiments have been carried out to verify that the THC passes through quasi-steady states when the freshwater flux is increasing. For diapycnal diffusivity 0.2 cm^2/s, the freshwater flux has been stabilized at 0.2 Sv and 0.3 Sv for 500 years. In both cases, the THC keeps on slowing down for about 100 to 150 years but it partially recovers and stabilizes within 300 years (not shown). Hence, the model can be considered to be in quasi-steady state for each value of the freshwater forcing. However, for sudden shifts in the regime of the circulation, the departure from equilibrium can be substantial. A slower rate of decrease in the freshwater flux would keep the model closer to equilibrium and avoid overshooting.

The ocean circulation becomes more sensitive to freshwater perturbations as the diapycnal diffusivity decreases, *i.e*. a smaller freshwater perturbation will cause the collapse of the thermohaline circulation. To the extent that global warming experiments lead to an increase of freshwater in the North Atlantic (Manabe and Stouffer, 1994), the latter statement could be extended to global warming experiments as well. The distance of the equilibrium climate from the instability threshold is different among different models. For models close to the threshold, changing the amount of freshwater input in the North Atlantic, as a consequence of global warming, may lead to a collapse of the THC and the shift to an equilibrium with no water sinking in the North Atlantic (Ganopolsky *et al*., 2001, their fig. 11).

6. CONCLUSIONS

We analyzed the sensitivity of the climate to diapycnal diffusivity for the equilibrium climate state. We focused particularly on the behavior of the THC and on vertical heat balance in the ocean. Additionally, a sensitivity study on the hysteresis cycle of the THC to the diapycnal diffusion is conducted with the MIT-EMIC. This study is unique because the sensitivity to diapycnal diffusion of the ocean has been investigated using a coupled model with a 3D ocean component.

For the present climate state, the strength of the THC in the North Atlantic scales with the 0.44 power of the diapycnal diffusivity whereas a simple theoretical model predicts a power of 2/3. The theoretical model assumes a vertical-diffusive balance in the ocean. Since the Pacific Ocean is about twice as large as the Atlantic Ocean most of the upwelling likely occurs in the former basin. Indeed, in our model, the Southern Pacific overturning scales with the 0.63 power of the diapycnal diffusivity. Hence, we suggest that a controlling factor of the THC strength, for a climate close to equilibrium, is the value of the diapycnal diffusivity in the Pacific basin.

At equilibrium, the vertical heat balance of the global ocean is sensitive to the diapycnal diffusivity. Weaker mixing in the ocean leads to smaller diapycnal diffusive fluxes in the tropics and a thinner thermocline. As a consequence, isopycnal slopes at high latitudes are gentler, leading to smaller isopycnal diffusive and bolus advective fluxes. Although the THC strength sensibly depends on the value of the diapycnal diffusivity, compensation between high latitude downwelling and tropical upwelling leads to small changes of the total vertical advective flux. The relative importance of the fluxes at high latitude, compared to the fluxes in the tropical region, depends on the diapycnal diffusivity — the main cause being the reduction of diapycnal diffusion in the tropics. For elevated diapycnal diffusivity, the tropics dominate the global balance and the advective-diffusive balance is valid at all depths. For reduced diapycnal diffusivity, high latitude processes are relatively more important than low latitude ones and, for the global ocean, the advective-diffusive balance is reversed in the upper 800m.

In addition, we performed a sensitivity test of the hysteresis curve to the diapycnal diffusivity. As suggested by previous studies with 2.5D coupled models and a 3D uncoupled model the THC becomes more unstable to freshwater perturbations for lower values of the diapycnal diffusivity. In 3D models, the threshold for the shutdown of the THC depends on the diapycnal diffusivity while in 2.5D models the same threshold is relatively insensitive to the diapycnal diffusivity. Less clear is the sensitivity of the threshold at which the circulation recovers from the "shutdown" mode. In the 3D uncoupled model of Prange *et al*. (2003) the above threshold slightly increases with decreasing diapycnal diffusivity. The opposite occurs for the MIT-EMIC and the 2.5D models. The gyre transport of salt in the North Atlantic, the atmosphere-ocean feedbacks and the non-linear dynamics are the major differences among the above models.

7. REFERENCES

Bryan, K., 1984: Accelerating the convergence to equilibrium of ocean-climate models. *Journal of Physical Oceanography*, **14**, 666-673.

Bryan, F., 1987: Parameter Sensitivity of Primitive Equation Ocean General Circulation Models. *Journal of Physical Oceanography*, **17**, 970-985.

Bugnion, V., and C. Hill, 2004a: Far field regulation of meridional overturning - the role of surface boundary conditions. *J. Climate*, in review.

Bugnion, V., and C. Hill, 2004b: An adjoint analysis of meridional overturning. *J. Climate*, in review.

Bugnion, V., and C. Hill, 2004c: Equilibration mechanisms in an adjoint ocean general circulation model. *Ocean Modeling*, in review.

Colin de Verdière, A., 1988: Buoyancy driven planetary flows. *J. of Marine Research*, **46**, 215-265.

Cummins, P. F., G. Holloway and A.E. Gargett, 1990: Sensitivity of the GFDL Ocean General Circulation Model to a Parameterization of Vertical Diffusion. *J. Phys. Ocean.*, **20**, 817-830.

Dalan, F., P. H. Stone and A. P. Sokolov, 2004: Sensitivity of Climate to Diapycnal Diffusivity in the Ocean. Part II: Global Warming Scenario. *Journal of Climate*.

Danabasoglu, G., and J. C. McWilliams, 1995: Sensitivity of the Global Ocean Circulation to Parameterizations of Mesoscale Tracer Transports. *Journal of Climate*, **8**, 2967-2987.

Ganachaud, A., and C. Wunsch, 2003: Large-scale Ocean Heat and Freshwater Transports During the World Ocean Circulation Experiment. *Journal of Climate*, **16**, 696-705.

Ganopolsky, A., V. Petoukhov, S. Rahmstorf, V. Brovkin, M. Claussen, A. Eliseev and C. Kubatzki, 2001: CLIMBER-2: a climate system model of intermediate complexity. Part II: model sensitivity. *Climate Dynamics*, **17**, 735-751.

Gent, P. R., and J.C. McWillams, 1990: Isopycnal Mixing in Ocean Circulation Models. *Journal of Physical Oceanography*, **20**, 150-155.

Gerdes, R., C. Köberle, and J. Willebrand, 1991: The influence of numerical advection schemes on the results of ocean general circulation models. *Climate Dynamics*, **5**, 211-226.

Gnanadesikan, A., 1999: A simple predictive model for the structure of the ocean pycnocline. *Science*, **283**, 2077-2079.

Gregory, J. M., 2000: Vertical heat transports in the ocean and their effect on time-dependent climate change. *Climate Dynamics*, **16**, 501-515.

Hansen, J., G. Russel, D. Rind, P. Stone, A. Lacis, S. Lebedeff, R. Ruedy and L. Travis, 1983: Efficient 3D global models for climate studies: Model I and II. *Monthly Weather Review*, **111**, 609-662.

Harvey, L. D. D., 1995: Impact of Isopycnal Diffusion on Heat Fluxes and the Transient Response of a Two-Dimensional Ocean Model. *Journal of Physical Oceanography*, **25**, 2166-2176.

Houghton, J. T., Y. Ding, D. J. Griggs, M. Noguer, P. J. van der Linden, X. Dai, K. Maskell and C. A. Johnson, 2001: *Climate Change 2001: The Scientific Basis.* Cambridge University press, 881 pp.

Huang, B., P. H. Stone and C. Hill, 2003: Sensitivities of deep-ocean heat uptake and heat content to surface fluxes and subgrid-scale parameters in an ocean general circulation model with idealized geometry. *Journal of Geophysical Research*, **108**, 3015, doi: 10.1029/2001JC001218.

Huang, R.X., 1999: Mixing and energetics of the oceanic thermohaline circulation. *Journal of Physical Oceanography*, **29**, 727-746.

Hughes, T.C.M., and A. J. Weaver, 1994: Multiple equilibria of an asymmetric two-basin ocean model. *Journal of Physical Oceanography*, **24**, 619-637.

Kamenkovich, I.V., J. Marotzke and P. H. Stone, 2000: Factors Affecting Heat Transport in an Ocean General Circulation Model. *Journal of Physical Oceanography*, **30**, 175-194.

Kamenkovich, I.V., A.P. Sokolov and P.H. Stone, 2002: An efficient climate model with a 3D ocean and a statistical-dynamical atmosphere. *Climate Dynamics*, **19**, 585-598.

Klinger, B. A., S. Drijfhout, J. Marotzke, and J. R. Scott, 2003: Sensitivity of basinwide meridional overturning to diapycnal diffusion and remote wind forcing in an idealized Atlantic-Southern Ocean geometry. *Journal of Physical Oceanography*, **33**, 249-266.

Knutti, R., T. F. Stocker and D. Wright, 2000: The Effects of Subgrid-Scale Parameterizations in a Zonally Averaged Ocean Model. *Journal of Physical Oceanography*, **30**, 2738-2752.

Ledwell, J. R., E. T. Montgomery, K. L. Polzin, L. C. St. Laurent, R. W. Schmitt & J. M. Toole, 2000: Evidence for enhanced mixing over rough topography in the abyssal ocean. *Nature*, **403**, 179-182.

Manabe, S., and R. J. Stouffer, 1994: Multiple-Century Response of a Coupled Ocean-Atmosphere Model to an Increase of Atmospheric Carbon Dioxide. *Journal of Climate*, **7**, 5-23.

Marotzke, J., 1997: Boundary Mixing and the Dynamics of Three-Dimensional Thermohaline Circulation. *Journal of Physical Oceanography*, **27**, 1713-1728.

Marotzke, J., and J. R. Scott, 1999: Convective Mixing and the Thermohaline Circulation. *Journal of Physical Oceanography*, **29**, 2962-2970.

Munk, W., 1966: Abyssal recipes. *Deep Sea Research*, **13**, 707-730.

Munk, W., and C. Wunsch, 1998: Abyssal recipes II: energetics of tidal and wind mixing. *Deep Sea Research*, **45**, 1977-2010.

Pacanowski, R. C., 1996: *MOM2 version 2.0: Documentation User's Guide and Reference Manual*. Geophysical Fluid Dynamics Laboratory, Technical Report 3.2, Princeton, New Jersey.

Park, Y. G., and K. Bryan, 2000: Comparison of Thermally Driven Circulations from a Depth-Coordinate Model and an Isopycnal-Layer Model. Part I: Scaling-Law Sensitivity to Vertical Diffusivity. *Journal of Physical Oceanography*, **30**, 590-605.

Polzin, K. L., J. M. Toole, J. R. Ledwell and R. W. Schmitt, 1997: Spatial Variability of Turbulent Mixing in the Abyssal Ocean. *Science*, **276**, 93-96.

Prange, M., G. Lohmann and A. Paul, 2003: Influence of Vertical Mixing on the Thermohaline Hysteresis: Analyses of an OGCM. *Journal of Physical Oceanography*, **33**, 1707-1721.

Prinn, R., H. Jacoby, A. Sokolov, C. Wang, X. Xiao, Z. Yang, R. Eckaus, P. Stone, D. Ellerman, J. Melillo, J. Fitzmaurice, D. Kicklighter, G. Holian & Y. Liu. Integrated Global System Model for Climate Policy Assessment: Feedbacks and Sensitivity Studies. *Climatic Change*, **41**, 469-546.

Redi, M. H., 1982: Oceanic isopycnal mixing by coordinate rotation. *J. Phys. Ocean.*, **12**, 1154-1158.

Samelson, R. M., 1998: Large-scale circulation with locally enhanced vertical mixing. *Journal of Physical Oceanography*, **28**, 712-726.

Schmittner, A., and A. J. Weaver, 2001: Dependence of multiple climate states on ocean mixing parameters. *Geophysical Research Letters*, **28**, 1027-1030.

Scott, J. R., 2000: *The Role of Mixing and Geothermal Heating and Surface Buoyancy Forcing in Ocean Meridional Overturning Dynamics*. Ph.D. thesis, Department of Earth, Atmospheric and Planetary Sciences, Massachusetts Institute of Technology, Cambridge, MA.

Scott, J. R., and J. Marotzke, 2002: The Location of Diapycnal Mixing and the Meridional Overturning Circulation. *Journal of Physical Oceanography*, **32**, 3578-3595.

Sokolov, A. P., and P. H. Stone, 1998: A flexible climate model for use in integrated assessments. *Climate Dynamics*, **14**, 291-303.

Stone, P. H., and M-S. Yao, 1990: Development of a Two-Dimensional Zonally Averaged Statistical-Dynamical Model. Part III: The Parameterization of the Eddy Fluxes of Heat and Moisture. *Journal of Climate*, **3**, 726-740.

Toggweiler, J. R., and B. Samuels, 1995: Effect of Drake Passage on the global thermohaline circulation. *Deep-Sea Research*, **42**, 477-500.

Toggweiler, J. R., and B. Samuels, 1998: On the ocean's large-scale circulation near the limit of no vertical mixing. *Journal of Physical Oceanography*, **28**, 1832-1852.

Thorpe, R. B., J. M. Gregory, T. C. Johns, R. A. Woods and J. F. B. Mitchell, 2001: Mechanisms Determining the Atlantic Thermohaline Circulation Response to Greenhouse Gas Forcing in a Non-Flux-Adjusted Coupled Climate Model. *Journal of Climate*, **14**, 3102-3116.

Vallis, G. K., 2000: Large-scale circulation and production of stratification: effects of wind, geometry, and diffusion. *Journal of Physical Oceanography*, **30**, 933-954.

Welander, P., 1971: The Thermocline Problem. *Philosophical Transactions of the Royal Society of London. Series A, Mathematical and Physical Sciences*, **270**, 415-421.

Wright, D. G., and T. F. Stocker, 1992: Sensitivities of a zonally averaged global ocean circulation model. *Journal of Geophysical Research*, **97**, 12707-12730.

Zhang, J., 1998: *Impacts of double-diffusive processes on the thermohaline circulation*. Ph.D. thesis, Massachusetts Institute of Technology and Woods Hole Oceanographic Institution, 157 pp.

Zhang, J., R. W. Schmitt and R. X. Huang, 1999: The Relative Influence of Diapycnal Mixing and Hydrologic Forcing on the Stability of the Thermohaline Circulation. *Journal of Physical Oceanography*, **29**, 1096-1108.

APPENDIX: A Convection-less Model

Convection in this version of the MIT-EMIC is almost negligible. In models with horizontal and vertical diffusion parameterizations convection is the only means by which heat can be transported efficiently from the deep ocean to the surface. With the recent introduction of Redi and Gent-McWilliams parameterizations (Redi, 1982; Gent and McWilliams, 1990), both isopycnal mixing and bolus velocities can efficiently mix the upper ocean, inhibiting convection. This effect has been noticed already in 2D (Harvey, 1995, fig. 2) and 3D ocean models (Danabasoglu and McWilliams, 1995, their fig. 22). In our model steeply sloping isopycnals are eliminated by using the tapering method of Gerdes *et al*. (1991), with a maximum slope of 0.01.

Reducing the isopycnal mixing and/or the bolus velocities would increase the ocean heat content and reduce the static stability. Convection should then be enhanced. To prove that this is the case, we have performed two additional equilibrium experiments. From the control run with diapycnal diffusion 0.5 cm^2/s, we spun up the coupled model in a separate experiment with the upper bound on the isopycnal slopes reduced from 0.01 in the standard model to 0.001, and in another experiment with the isopycnal diffusivity reduced from 1000 m^2/s to 100 m^2/s.

In the Reduced-Maximum-Slope (RMS) case, the maximum overturning in the Atlantic increases 2 Sv in comparison with the standard model (26 Sv), while the temperature structure is almost unchanged. Moreover, the GM streamfunction is reduced in the Southern Ocean but almost canceled in the North Atlantic, going from a maximum of 15 Sv to less that 4 Sv (**Figure A1**a, b).

In the Small-Isopycnal-Diffusion (SID) case, the maximum overturning in the North Atlantic decreases by 2 Sv and the whole ocean warms up. The GM streamfunction is reduced by about 4 Sv, against the 11 Sv reduction of the RMS case (Fig. 1a and c). The introduction of the GM mixing scheme has been shown in the past to improve the representation of the ocean circulation mainly in the Southern Ocean (Danabasoglu and McWilliams, 1995, their figs. 4 and 5), thus a distribution of the bolus velocities as in the RMS case, with larger velocities in the Southern Ocean than in the Northern Ocean, agrees better with that reported in 3D GCMs with realistic geometry (Danabasoglu and McWilliams, 1995).

The heat balance of the Atlantic Ocean only is presented in **Figure A2**. In the RMS case both the isopycnal diffusive flux and GM advective flux are about half the control run fluxes (Fig. A2a and b). Compensating the reduction of these fluxes, a reduction of diapycnal diffusive fluxes and the appearance of upward convective fluxes is observed. Eulerian advection is virtually unchanged. In the SID case, the isopycnal diffusive fluxes decrease considerably, balancing the reduction of diapycnal diffusion (Fig. A2a and c). Convection plays a minor but not negligible role in the balance, while eulerian advection slightly increases at every depth level.

This result confirms that convective fluxes in the standard version of our model are being inhibited by GM advective fluxes and isopycnal diffusive fluxes. Greatly reducing the isopycnal diffusion only allows for convection to constitute a small term in the heat balance. However, reducing both isopycnal diffusion and GM advection by roughly 50% (accomplished by reducing the maximum slope of isopycnals) strongly enhances convective mixing. Therefore, we suggest that the GM fluxes are more efficient than the isopycnal fluxes in increasing the stability of the water column. Changing the isopycnal diffusivity and the maximum isopycnal slope involves also changes in the circulation pattern as well as in the surface heat flux distribution.

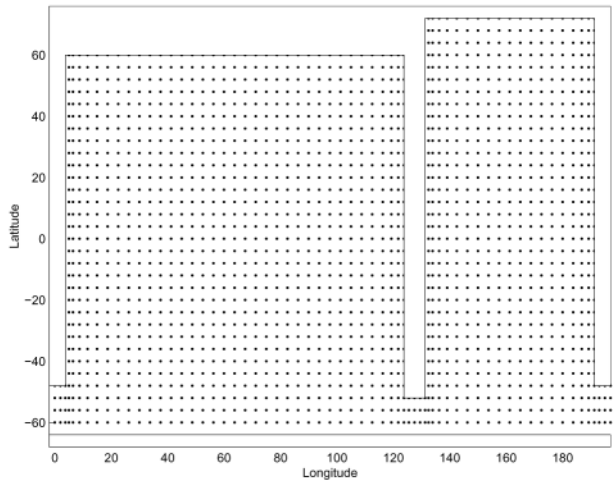

Figure 1: Geometry of the ocean model and velocity points in the Arakawa B-grid.

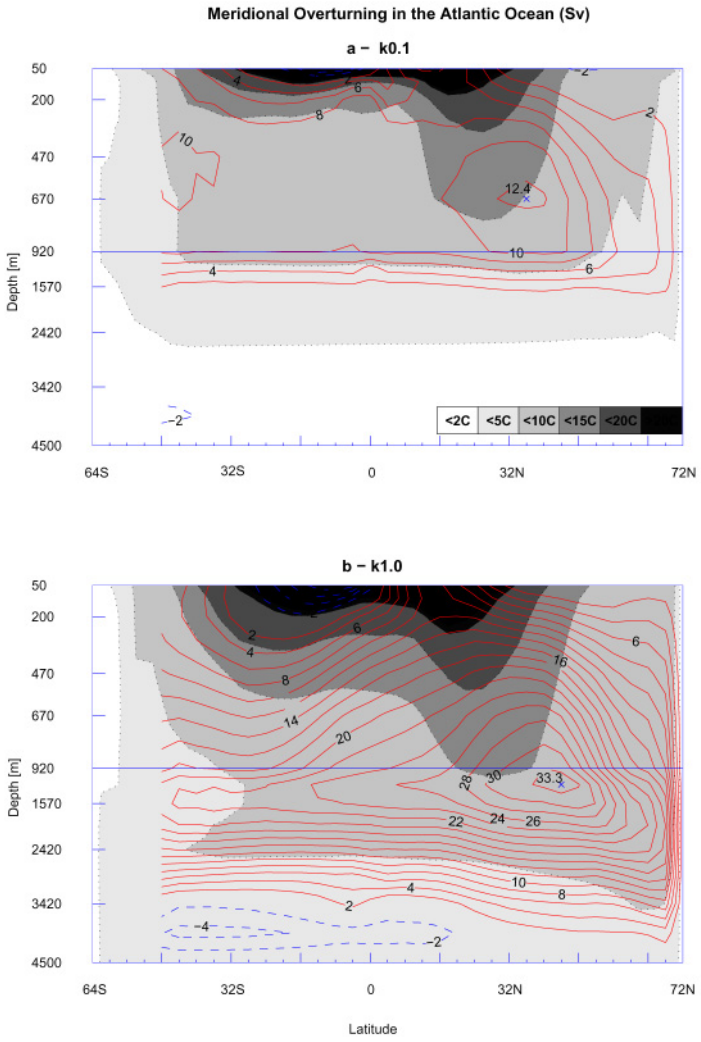

Figure 2: Meridional streamfunction of the Atlantic Ocean at equilibrium for diapycnal diffusivity **(a)** 0.1 cm^2/s and **(b)** 1.0 cm^2/s. Solid line for clockwise overturning and dashed line for anticlockwise overturning. Shading indicates temperature according to the scale in panel a.

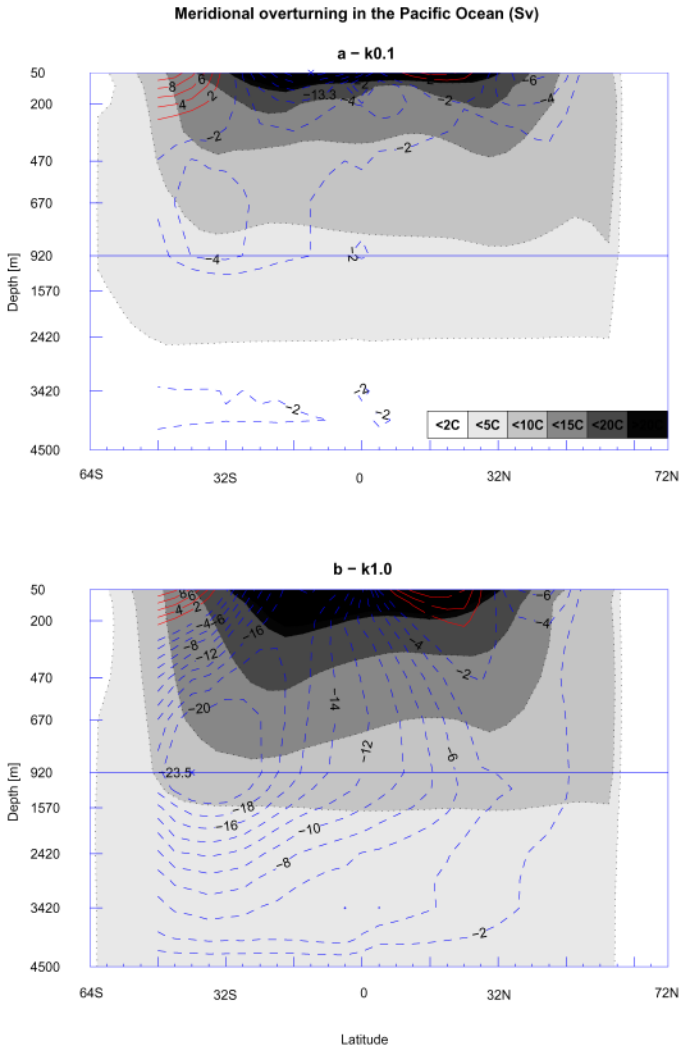

Figure 3: Meridional streamfunction of the Pacific Ocean at equilibrium for diapycnal diffusivity **(a)** 0.1 cm^2/s and **(b)** 1.0 cm^2/s. Solid line for clockwise overturning and dashed line for anticlockwise overturning. Shading indicates temperature according to the scale in panel a.

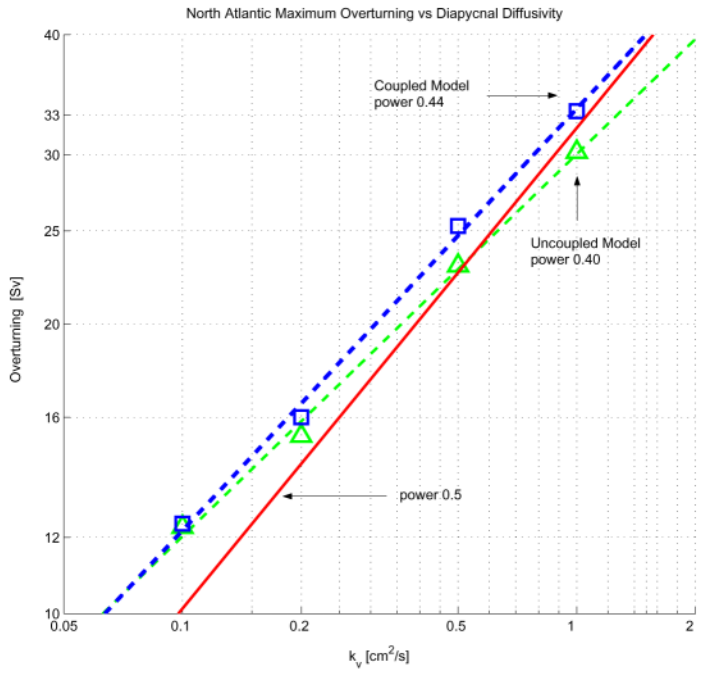

Figure 4: Maximum in the meridional streamfunction of the North Atlantic Ocean for coupled (squares) and uncoupled (triangles) model at equilibrium versus diapycnal diffusivity (k_v). Log-Log plot. Linear regression lines are dashed while the solid line shows threlation $(k_v)^{0.5}$ for comparison.

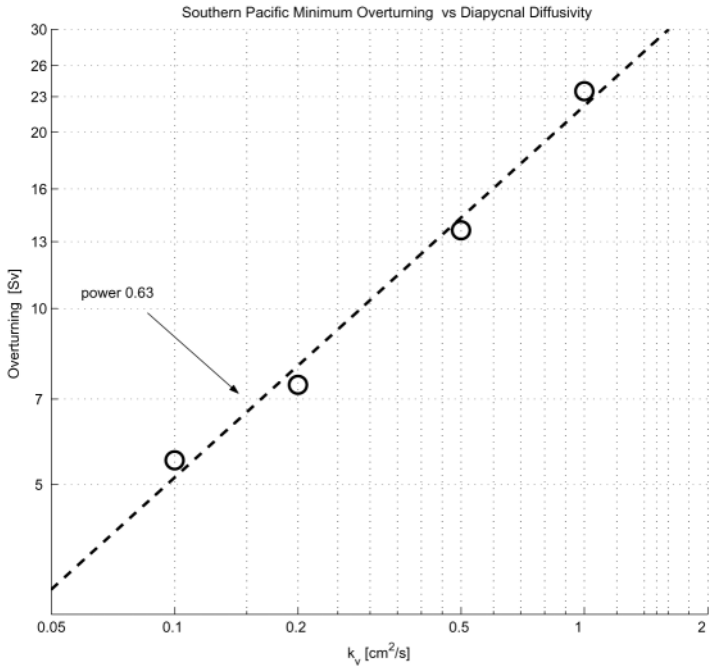

Figure 5: Minimum in the meridional streamfunction of the South Pacific Ocean (circles) at equilibrium versus diapycnal diffusivity (k_v). Log-Log plot. Linear regression line is dashed.

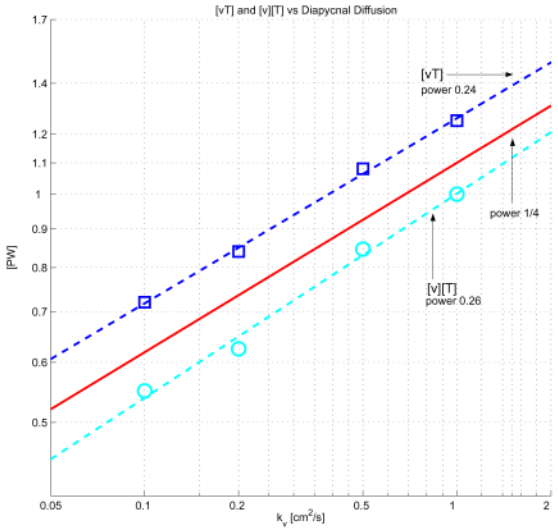

Figure 6: Maximum poleward heat transport ([vT], squares) and heat transport by the mean meridional circulation ([v][T], circles) for the global ocean at equilibrium versus diapycnal diffusivity (k_v). Log-Log plot. Both [v] and [T] are normalized by their value at diffusivity 1.0 cm^2/s. Linear regression lines are dashed while the solid line represent the relation $(k_v)^{0.25}$.

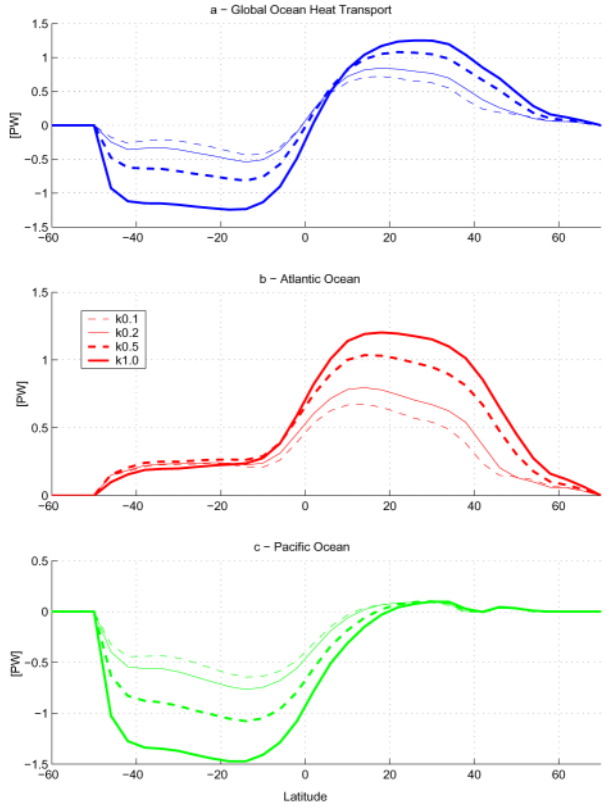

Figure 7: Poleward heat transport for **(top)** the global ocean, **(middle)** Atlantic Ocean, and **(bottom)** Pacific Ocean for diapycnal diffusivity 0.1 cm^2/s (thin dashed line), 0.2 cm^2/s (thin solid line), 0.5 cm^2/s (thick dashed line) and 1.0 cm^2/s (thick solid line).

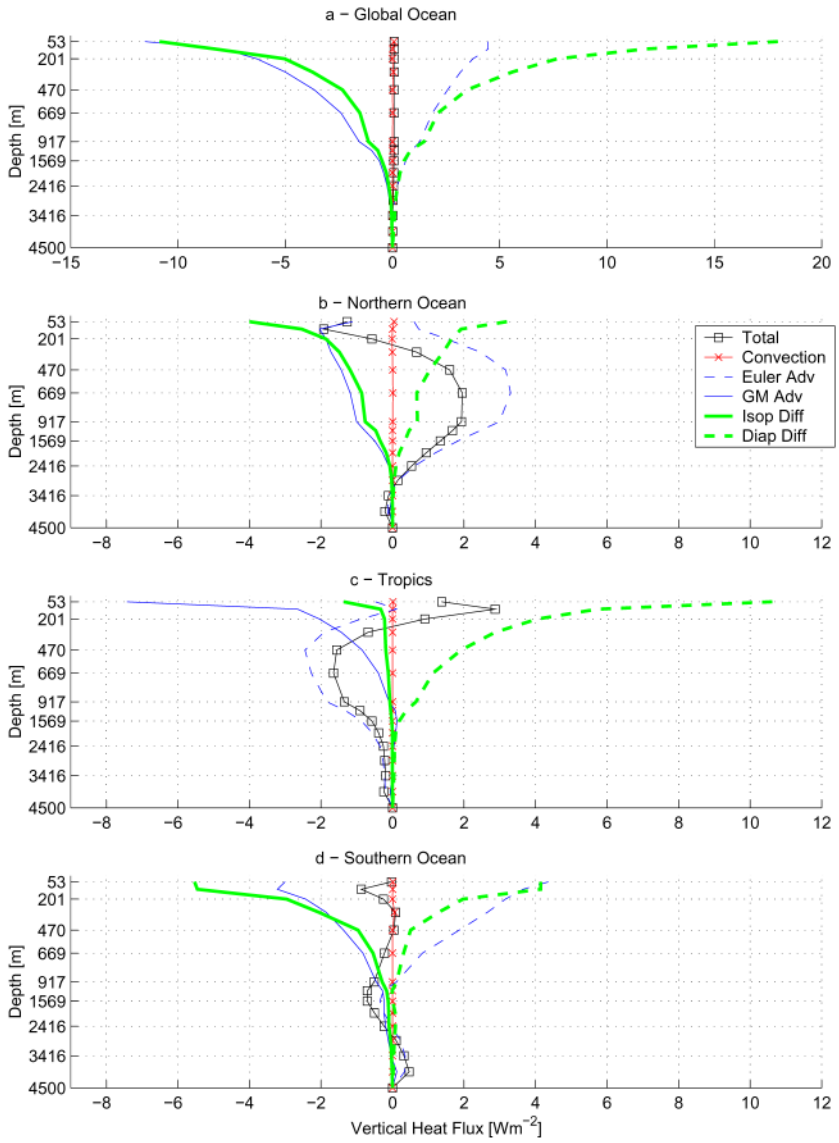

Figure 8: Vertical heat flux components for **(a)** global ocean, **(b)** Northern Ocean, **(c)** Tropics, and **(d)** Southern Ocean for diapycnal diffusivity 0.5 cm^2/s. Positive (negative) sign for downward (upward) fluxes. Note the change of scale in panel a.

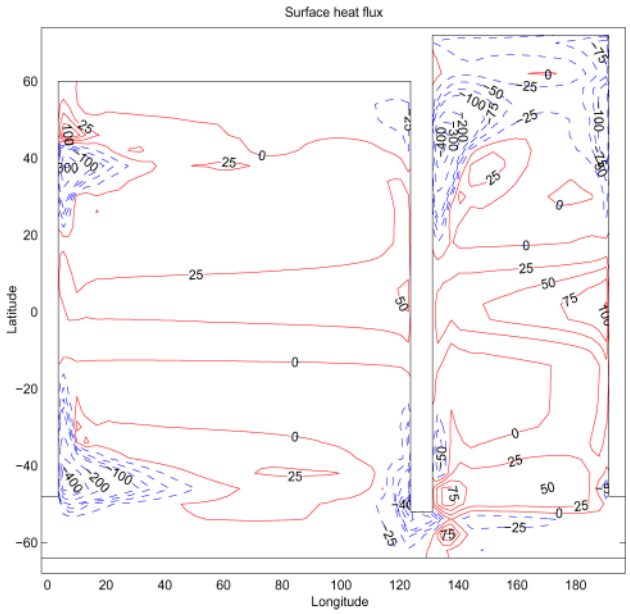

Figure 9: Surface heat flux in Wm^{-2} for diapycnal diffusivity 0.5 cm^2/s. Contour interval is 25 Wm^{-2} between values of –100 Wm^{-2} to 100 Wm^{-2}, and 100 Wm^{-2} outside this range. Solid (dashed) line for positive (negative) values.

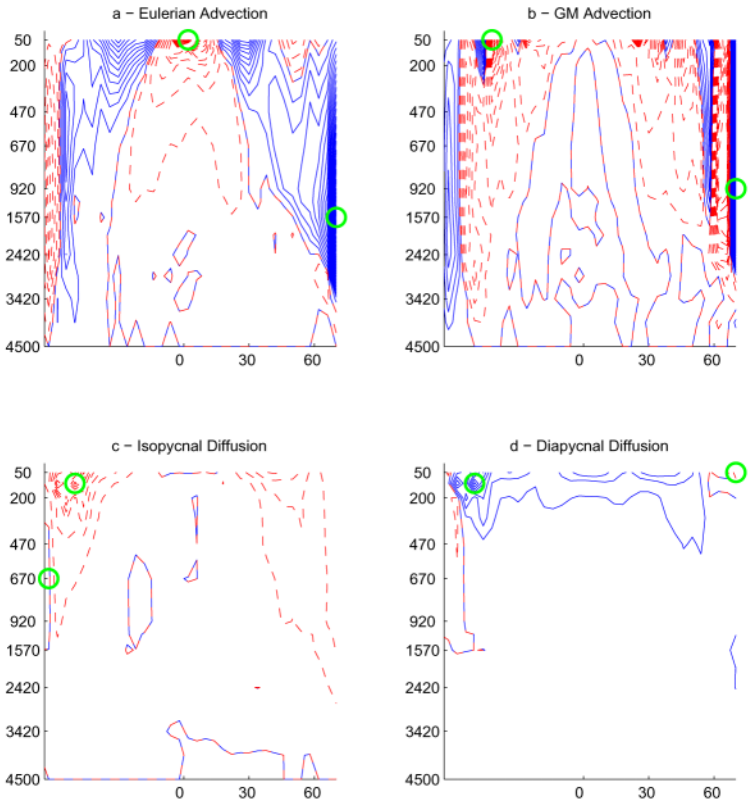

Figure 10: Zonally averaged vertical heat flux components for global ocean and diapycnal diffusivity 0.5 cm^2/s: **(a)** eulerian advection, **(b)** GM advection, **(c)** isopycnal diffusion and **(d)** diapycnal diffusion. Solid (dashed) line for downward (upward) fluxes. Circles denote the position of the maximum and minimum.

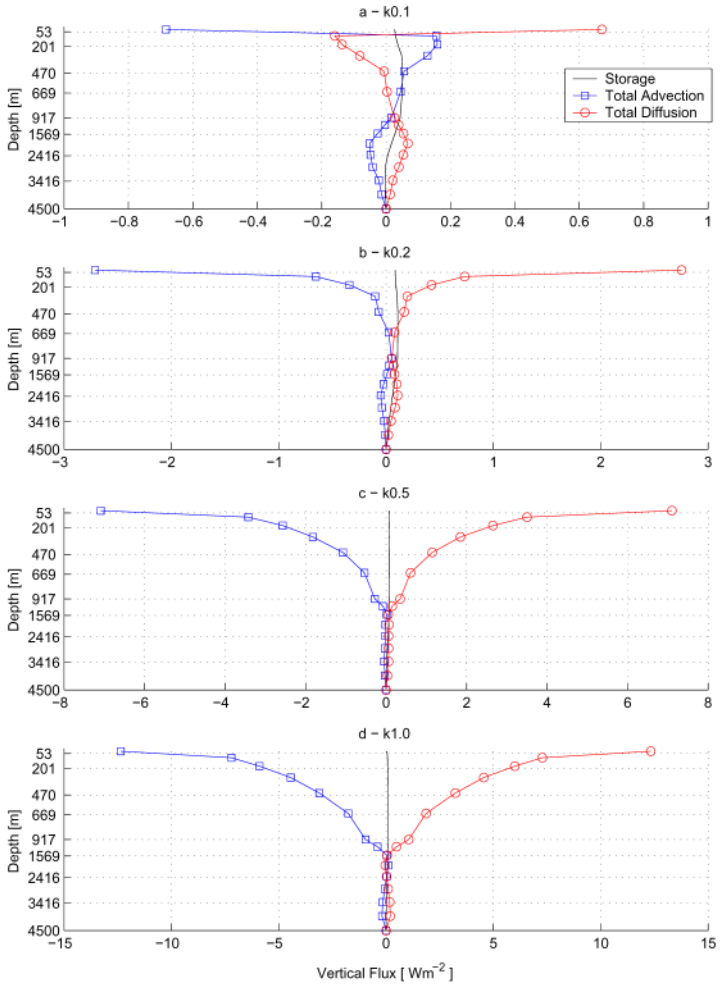

Figure 11: Heat balance for the global ocean for diapycnal diffusivity **(a)** 0.1 cm^2/s, **(b)** 0.2 cm^2/s, **(c)** 0.5 cm^2/s and **(d)** 1.0 cm^2/s. Positive (negative) sign for downward (upward) fluxes. Note the change in horizontal scales.

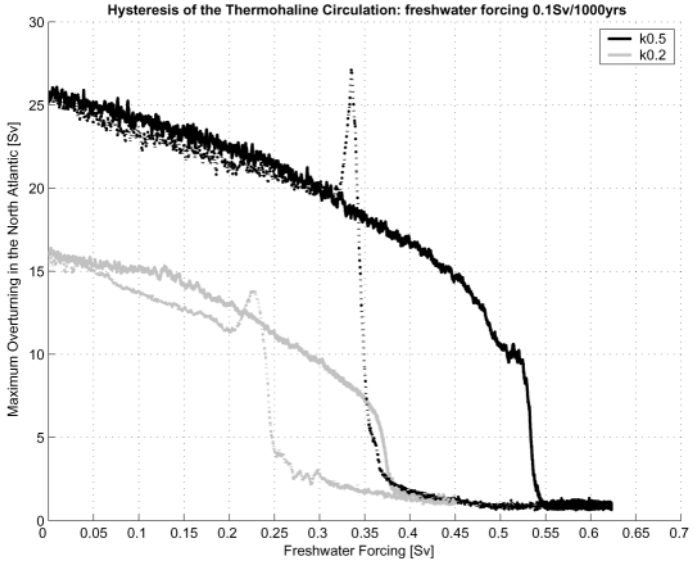

Figure 12: Hysteresis cycle of the THC for diapycnal diffusivity 0.5 cm^2/s and 0.2 cm^2/s.

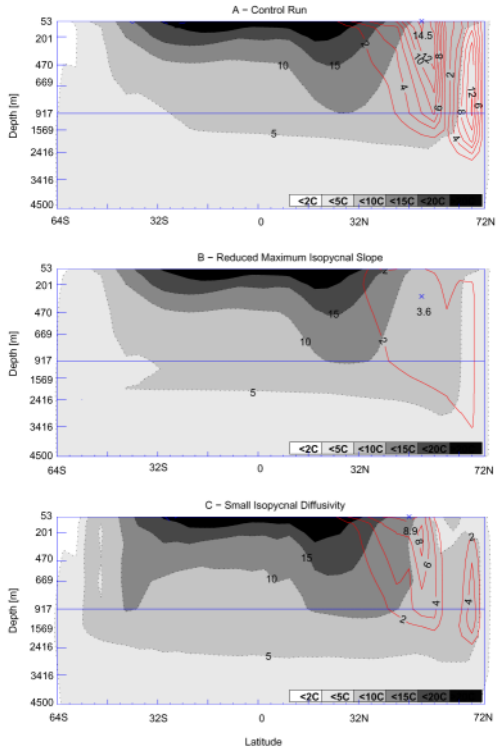

Figure A1: Bolus velocity streamfunction in the Atlantic Ocean for diapycnal diffusivity 0.5 cm^2/s. **(a)**Control run, **(b)** Reduced Maximum isopycnal Slope, and **(c)** Small Isopycnal Diffusivity experiments. Zonal average temperature is shaded according to the scale in panel a.

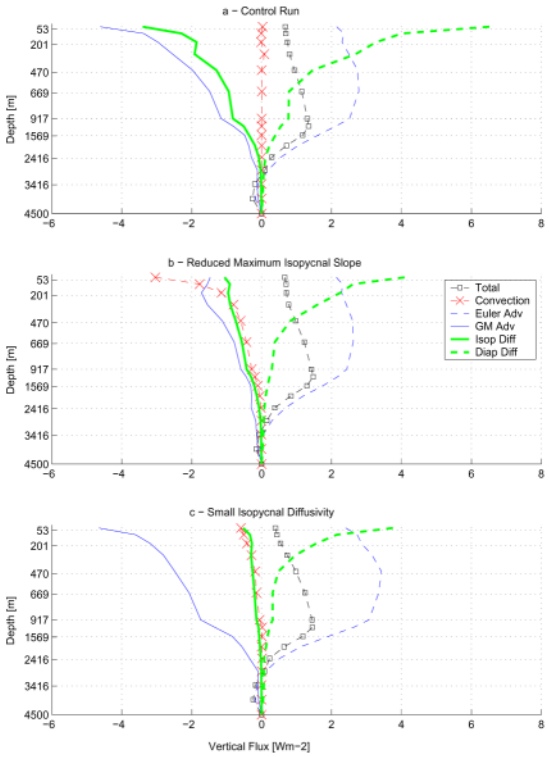

Figure A2: Vertical heat balance in the Atlantic Ocean for diapycnal diffusivity 0.5 cm^2/s. **(a)**Control run, **(b)** Reduced Maximum isopycnal Slope, and **(c)** Small Isopycnal Diffusivity experiments.

Sensitivity of Climate to Diapycnal Diffusivity in the Ocean Part II: *Global Warming Scenario*

Fabio Dalan[*], Peter H. Stone[†] and Andrei Sokolov[†]

Abstract

The sensitivity of the transient climate to the diapycnal diffusivity in the ocean is studied for a global warming scenario in which CO_2 increases by 1% per year for 75 years. The thermohaline circulation slows down for about 100 years and recovers afterward, for any value of the diapycnal diffusivity. The rates of slowdown and of recovery, as well as the percentage recovery of the circulation at the end of 1000-year integrations, are variable but a direct relation with the diapycnal diffusivity cannot be found. At year 70 (when CO_2, has doubled) an increase of the diapycnal diffusivity from 0.1 cm^2/s to 1.0 cm^2/s leads to a decrease in surface air temperature of about 0.4 K and an increase in sea level rise of about 4 cm The steric height gradient is divided into thermal component and haline component. It appears that, in the first 60 years of simulated global warming, temperature variations dominate the salinity ones in weakly diffusive models, whereas the opposite occurs in strongly diffusive models.

The analysis of the vertical heat balance reveals that deep ocean heat uptake is due to reduced upward isopycnal diffusive flux and Gent-McWilliams advective flux. Surface warming, induced by enhanced CO_2 in the atmosphere, leads to a reduction of the isopycnal slope which translates into a reduction of the above fluxes. The amount of reduction is directly related to the magnitude of the isopycnal diffusive flux and GM advective flux at equilibrium. These latter fluxes depend on the thickness of the thermocline at equilibrium, hence on the diapycnal diffusion. Thus, the increase of deep-ocean heat uptake with diapycnal diffusivity is an indirect effect that the latter parameter has on the isopycnal diffusion and GM advection.

Contents

1. INTRODUCTION

Climate models are very sensitive to the diapycnal diffusivity, both for the equilibrium climate state (Bryan, 1987; Marotzke, 1997; Zhang *et al*., 1999; Park and Bryan, 2000) and in transient experiments, triggering strong non-linear behavior (Ganopolsky *et al*., 2001; Manabe and Stouffer, 1999). Yet, the global averaged value of the diapycnal diffusivity is uncertain. Measurements of

[*] Corresponding author. Postal address: Via Cavour 44/e, 35030 Rubano (PD), Italy. Tel: +39 049 328 47 80 663. Email: fabio.dalan@alum.mit.edu

[†] Joint Program on the Science and the Policy of Climate Change, MIT, Cambridge, Massachusetts, USA

the diapycnal diffusivity are localized in space and time (Polzin *et al*., 1997; Ledwell *et al*., 2000) while calculations of the global averaged diapycnal diffusivity vary as much as a factor 5 (Munk and Wunsch, 1998; Huang, 1999). In Part I of this study we analyzed the sensitivity of the current climate to the diapycnal diffusivity (Dalan *et al.*, 2004). In this paper we illustrate the influence of the diapycnal diffusivity on the transient behavior of the thermohaline circulation (THC) and on the rate of change of heat content, sea surface temperature and sea level rise.

The THC appears to be driven by the steric height gradient between North and South Atlantic (Hughes and Weaver, 1994). By changing the relative strength of the processes transporting heat and salt in the ocean, positive feedbacks may strengthen, triggering strong non-linear behavior in the THC evolution. By changing the rate of CO_2 increase in the atmosphere, Stocker and Schmittner (1997) observed a slowdown and recovery of the THC or a complete collapse of the THC for slow and fast rates respectively. The same pattern was observed by Ganopolsky *et al*. (2001) varying both vertical diffusivity and hydrological sensitivity in a 2.5D ocean model coupled with a 2D statistical-dynamical model. For low vertical diffusivity and high hydrological sensitivity the THC shuts down in a simulation with 1% CO_2 rate of increase for 140 years and constant afterwards (stabilization at 4 x CO_2). For all the other combinations of the two parameters the strength of the THC decreases for about 150 years and then partially recovers. This study will extend Ganopolsky *et al.* (2001) results by using a 3D ocean model coupled with a 2D atmosphere and varying only the diapycnal diffusivity. Furthermore, the change in steric height gradient is divided into thermal component and haline component and the relative magnitude of the components is analyzed with respect to changes in the diapycnal diffusivity.

In the last IPCC report (Houghton *et al.* , 2001), the results from model projections of leading research groups are presented. Among other quantities, models are commonly compared in terms of surface air temperature (SAT) change and sea level rise (SLR). All models simulate an increase in surface air temperature and sea level, as a consequence of an increase of CO_2 in the atmosphere, but the magnitude of the increase varies as much as a factor of three. Both SAT and SLR due to thermal expansion depend on the rate of deep ocean heat uptake. The rate of increase of SAT depends on the effective heat capacity of the Earth system. Because of the large heat capacity of water compared to air and land, the heat capacity of the combined atmosphere-land-ocean system depends on the portion of ocean that will be affected by global warming, therefore on the rate of ocean heat uptake. The sea level rises mainly because the volume of the water increases with temperature, therefore it also depends on the rate at which the ocean takes up heat.

The rate of ocean heat uptake is not well constrained by observations of the temperature record of the past 50 years (Forest *et al*., 2002) and varies greatly among models (Sokolov *et al*., 2003). Hence, detailed studies on the vertical heat balance in the ocean are needed in order to understand which processes and parameters control the rate of ocean heat uptake in numerical models. Two studies of this kind are presented by Gregory (2000) and Huang *et al*. (2003c). In the first study advective fluxes (eulerian and bolus velocity advection) and diffusive fluxes

(isopycnal and diapycnal) are combined together, when analyzing the global ocean balance, and the balance for different latitude bands and basins is limited to a single depth level (160 m). We will hereafter refer to the bolus advective flux as the GM flux. Huang *et al*. (2003a, b, c) combine together the isopycnal diffusive flux and the GM flux. Their adjoint sensitivity studies show that the heat content of the ocean and its change in transient climate scenarios is dependent on these combined fluxes (Huang *et al.*, 2003a and b). However, varying both the isopycnal and thickness diffusivities simultaneously does not change appreciably the rate of ocean heat uptake (Huang *et al*., 2003c). In this paper, the vertical heat flux of the ocean is divided into all its components and for every depth level. Moreover the sensitivity of the rate of deep ocean heat uptake to diapycnal diffusivity is presented for a standard global warming scenario. For the sensitivity of the vertical heat balance at equilibrium refer to Dalan *et al*. (2004).

Uncertainty in the heat uptake is a major source of uncertainty in global warming projections (Webster *et al.*, 2003). Sokolov *et al*. (2003) found the difference in the heat uptake simulated by coupled atmosphere-ocean GCMs (AOGCMs) could be described by differences in the rate at which heat anomalies are effectively diffused into the ocean. Using the Sokolov *et al*. (2003) model to fit the trend of the MIT-EMIC, we will relate the diapycnal diffusivity to the effective vertical diffusivity of Sokolov *et al*. (2003).

The paper is organized as follow: in Section 2 we briefly describe the numerical model; in Section 3 we analyze the transient behavior of the THC circulation for simulations with different diapycnal diffusivity; Section 4 contains the sensitivity of the ocean heat uptake, SAT and SLR to the diapycnal diffusivity; finally, Section 5 contains a review of the results.

2. MIT EARTH MODEL OF INTERMEDIATE COMPLEXITY

More details of the model can be found in Kamenkovich *et al*. (2002).

2a. Atmospheric component

The 2-dimensional zonally averaged statistical-dynamical atmospheric model was developed by Sokolov and Stone (1998) on the basis of the GISS GCM (Hansen *et al*., 1983). The model solves the zonally averaged primitive equations in latitude-pressure coordinates. The grid of the model consists of 24 points in the meridional direction, corresponding to a resolution of 7.826°, and 9 layers in the vertical. Moreover, the model includes the parameterization of heat, moisture and momentum transports by large scale eddies (Stone and Yao, 1990) and has a complete moisture and momentum cycle.

Most of the physics and parameterizations of the atmospheric model derive from the GISS GCM. The 2D model, as well as the GISS GCM, allows four different types of surfaces in the same grid cell, namely: open ocean, sea-ice, land, and land-ice. The surface characteristics, as well as turbulent and radiative fluxes, are calculated separately for each kind of surface, while the atmosphere above is assumed to be well-mixed zonally. The atmospheric model uses a realistic land/ocean ratio at each latitude band. More detailed description of this part of the model can be found in Sokolov and Stone (1998) and Prinn *et al*. (1999).

The dependence of zonal-mean surface fluxes of heat and momentum on surface warming simulated by this model coupled to a 2D ocean model is similar to that shown by more sophisticated atmospheric GCMs (Sokolov and Stone, 1998; Prinn *et al.*, 1999). Moreover, vertical and latitudinal structure of the 2D model response is also consistent with the results of different GCMs. However, such a model cannot represent feedbacks associated with changes in the ocean circulation. To take into account possible interactions between atmosphere and ocean circulation, the 2D ocean model is replaced, in this study, by a 3D ocean GCM with simplified geometry.

2b. Ocean component

The ocean component of the coupled model is the MOM2 model (Pacanowski, 1996) with idealized geometry. It consists of two rectangular "pool" basins connected by a Drake Passage that extends from 64°S to 52°S. The Indo-Pacific (hereinafter Pacific) pool extends from 48°S to 60°N and is 120° wide while the Atlantic pool extends from 48°S to 72°N and is 60° wide. The meridional resolution is 4° and the zonal resolution varies from 1° near the north-south boundaries to 3.75° in the interior of the ocean. In the vertical, the model has 15 layers of increasing thickness from 53 m at the surface to 547 m at depth. The bottom of the ocean is flat and 4500 m deep everywhere except in the Drake Passage where there is a sill 2900 m deep.

No-slip boundary conditions are applied to the lateral walls and free-slip boundary conditions at the bottom of the ocean, except in the Antarctic Circumpolar Current (ACC) where bottom drag exists. Boundary conditions for tracers are insulating at lateral walls and bottom of the ocean. A mixed layer model adopted from the GISS GCM replaces the Ocean GCM southward of 64°S and northward of 72°N. The depth of the mixed layer is prescribed from observations as a function of latitude and time. In climate change simulations, heat penetrating into the ocean below the mixed layers is parameterized by diffusion of the deviation of the mixed layer temperature from its present-day climate values. Moreover, any changes in the runoff are evenly distributed throughout the ocean at any given time.

The Gent McWilliams parameterization scheme is used to account for the small scale eddy induced transport (Gent and McWilliams, 1990). Mixing caused by small scale processes occurs along and across isopycnals (Redi, 1982). No background horizontal diffusivity is used. The surface boundary conditions used to spin up the ocean model are taken from Jiang *et al*. (1999) who constructed the datasets using a variety of sources.

2c. Coupling, Spinup and Experiments Setup

Coupling takes place twice a day. The atmospheric model calculates 12-hour mean values of the wind stress, heat and freshwater fluxes over the open ocean and their derivatives with respect to the sea surface temperature (SST). These quantities are then linearly interpolated to the oceanic grid. The derivatives of the surface fluxes with respect to the SST are multiplied by the deviation of the SST from its zonal mean. This term is then added to the atmospheric surface

fluxes and passed to the ocean model. This procedure allows one to account for the zonal variations of the surface fluxes. The coupling procedure uses flux adjustments. The adjustments are given by the difference between the surface fluxes diagnosed after the spinup of the ocean-only model and the fluxes generated in the spinup of the atmospheric model alone forced by observed SST and sea-ice distribution. Wind stress adjustments are calculated in the same way. The ocean is integrated for 12 hours and provides to the atmosphere the zonal mean SST. Asynchronous integration is used (Bryan, 1984), with 12 hour time-step for the tracer equations and 1 hour time-step for the momentum equations. For more details on the coupling procedure see Dalan *et al*. (2004).

After separate spinup of the atmospheric and oceanic components the model has been coupled and spun up for 1000 years for each value of the diapycnal diffusivity: 0.1, 0.2, 0.5 and 1.0 cm^2/s. The model was considered to be at equilibrium when the global average heat flux entering the ocean fluctuates around the zero value. In the global warming experiments, the CO_2 in the atmosphere increases by 1% per year for 75 years and then it is kept constant for 925 years. Control runs are also performed starting at the end of the coupled spinup, with constant CO_2 concentration for 1000 years. As a measure of the transient climate change at the time of CO_2 doubling we take the difference between the mean climate in the global warming experiments and the control climate averaged over years 66 to 75.

3. BEHAVIOR OF THE THERMOHALINE CIRCULATION

In our model the thermohaline circulation slows down as a consequence of enhanced CO_2 in the atmosphere (**Figure 1**), as it does in most CMIP2 models. For each global warming simulation with different diapycnal diffusivity, the strength of circulation in the Atlantic Ocean decreases for 100 years, 25 years after the stabilization of the CO_2, and it recovers afterwards. Hence, the behavior of the system to changes in diapycnal diffusivity is self-similar. Ganopolsky *et al*. (2001) found strong non-linear behavior of the THC varying both vertical diffusivity and hydrological sensitivity. For small vertical diffusivity and large hydrological sensitivity the THC shuts down for a 1% CO_2 increase for 140 years, while for all other combinations of the two parameters the THC slows down and then partially recovers. Our model is extremely stable to freshwater perturbations, as inferred from the hysteresis curves presented in Dalan *et al*. (2004). Moreover, we do not register major changes in freshwater flux in the North Atlantic as a consequence of global warming (Kamenkovich *et al*., 2003).

The rate and the amount of recovery vary for each experiment in an unpredictable way. For example, the simulation with diffusivity 0.5 cm^2/s presents the fastest recovery although it is with the diffusivity 0.2 cm^2/s that the circulation first fully recovers its strength (Fig. 1). Moreover, the natural variability of the THC in the control run increases with the diapycnal diffusivity, its value going from 0.2 Sv for the 0.1 cm^2/s diffusivity to 1 Sv for the 1.0 cm^2/s diffusivity. The behavior of the circulation depicted in Fig. 1 raises the question of the

predictability of the THC in global warming experiments (Knutti and Stocker, 2002). Regardless of the path followed in the recovery, the new equilibrium achieved after the CO_2 stabilization, presents a shallower overturning circulation (not shown), as noted by Huang *et al*. (2003c). As a consequence of the THC slowdown, the bottom of the ocean fills up with cold water, which represents an obstacle for the water sinking in the North Atlantic when the circulation recovers.

The steric height is the integrated pressure from the surface to a reference depth, hence it is proportional to the quantity:

$$P = \int_{z^*}^{0} \int_{z}^{0} \frac{\rho}{\rho_o} dz' dz$$

where ρ is the in-situ density, ρ_0 is a reference density and z* is a reference depth, in our case 3000 m. The THC strength at equilibrium is correlated to the steric height difference between the North and South Atlantic (Hughes and Weaver, 1994; Thorpe *et al*., 2001). In the idealized geometry of the MIT-EMIC, the steric height difference is not sensitive to the choice of the South Atlantic latitude, as long as the latter is located northward of the Drake Passage, while the North Atlantic latitude needs to be north of 60°N. The THC strength at equilibrium is best correlated to the steric height difference in the Atlantic Ocean when the latter is calculated between 30°S and 66°N to 70°N. Since the THC circulation is stronger for increasing diapycnal diffusivity, the Gulf Stream extends to higher latitudes for models with 0.5 and 1.0 cm^2/s diapycnal diffusivity. Hence, for a fair comparison among simulations with different diapycnal diffusivity, the steric height is calculated between 30°S and 66°N for diffusivities 0.1 and 0.2 cm^2/s and between 30°S and 70°N for diffusivities 0.5 and 1.0 cm^2/s.

Both the percentage reduction of the THC strength and steric height gradient decrease with increasing overturning (**Figure 2**). However the steric height gradient change does not correlate with the percentage recovery at the end of the integration. This indicates that the longitudinal variations of the steric height may be relevant to explain the transient behavior of the THC.

Since the steric height depends on the density of the water column, we want to quantify the relative importance of the temperature and salinity profile in determining the steric height gradient. Using the temperature field from the transient run and the salinity field from the control run, we can calculate the temperature contribution to the steric height gradient. The salinity contribution is computed with the same technique. The result is depicted in **Figure 3**. For all simulations, the timeseries of the temperature and salinity contribution to the steric height gradient anomaly have a common trend, summarized as follows: at first, both temperature and salinity contributes to the decrease of the steric height gradient, while, after a certain time, temperature and salinity have opposite contributions to the steric height gradient (Fig. 3). The time at which the rate of change of the salinity contribution becomes positive is roughly 140 years for the smallest diffusivities (0.1 and 0.2 cm^2/s) and 70 years for the largest diffusivities (0.5 and 1.0 cm^2/s). Therefore we can identify two types of systems: a slow responding system for small diffusivities and a fast responding system for large diffusivities.

An important characteristic of the response of the system is the relative role of temperature and salinity in determining the steric height gradient in the first 75 years of the transient runs. For slow responding systems, the temperature effect is always the dominant term (Fig. 3a and b). For fast responding systems, in the first decades of integration, the salinity anomalies have greater importance (Fig. 3c and d) than the temperature anomalies in determining the steric height gradient. At the time of doubling of CO_2 however, the changes in the temperature distribution in the ocean are driving the steric height gradient for all the global warming simulations.

Thorpe *et al*. (2001) carried out a detailed analysis of the changes in steric height gradient. The authors concluded that, in the first 70 years of global warming, at the surface fluxes of heat and freshwater tend to slowdown the THC, while the changes in the meridional heat and salt transport help the THC recovery. An examination of our results suggests that the salinity fluxes in the deep ocean are dominated by advection, both in the equilibrium and transient experiments. For the temperature contribution the situation is more complicated. Changes in the GM advection and isopycnal diffusion tend to warm the North Atlantic as we will see in the next section. Moreover, the reduction of the THC implies a substantial reduction of the heat transport into high latitudes. This leads to a relative cooling of the North Atlantic and warming of the tropical Atlantic. Hence, changes in both GM advection and isopycnal diffusion decrease the steric height gradient while the decrease in meridional heat transport tends to increase it. Additionally, the density contribution of the heat flux at the surface in the North Atlantic in our model is about 7 times larger than the freshwater flux as shown by Kamenkovich *et al*. (2003, their figures 2a and 3).

The climate is a potentially chaotic system, therefore the realizations portrayed in Fig. 3 may depend on the initial condition. To further investigate this aspect, we perform another global warming experiment with diapycnal diffusivity 0.5 cm^2/s starting from year 10 of the control run. Starting from a different initial condition slightly changes the relative importance of temperature and salinity in the first 70 years of integration (not shown). In particular, in one case the salt component of the steric height anomaly is larger than the temperature component for about 65 years of global warming; in the other case the dominance of the salt component extends shortly over 70 years of integration.

A direct consequence of our observations is that models with large equilibrium THC overturning may be more sensitive to changes in the salt content in the North Atlantic, as a consequence of enhanced CO_2 in the atmosphere. Hence, even for models showing the same surface heat and freshwater flux perturbations under global warming experiments, the sensitivities to the surface forcing may be different.

4. VERTICAL HEAT IMBALANCE

The ocean heat uptake is an important factor in controlling the behavior of the THC under global warming experiments because it affects the temperature, and therefore the density, structure of the ocean. Hence, investigating the relationship between ocean heat uptake and

diapycnal diffusivity may give some insight on the behavior of the THC under global warming experiments. In the previous section we have seen how the competition between temperature and salinity, in determining the steric height gradient, is affected by the diapycnal diffusivity. Here, we investigate which processes are responsible for the temperature change in the deep ocean as the CO_2 increases in the atmosphere, and what is their relation with respect to the diapycnal diffusivity. Addressing these questions can help us understand whether differences in diapycnal diffusivity is one reason for the disagreement among IPCC models in the matter of surface air temperature and sea level rise.

4a. Global Warming Experiment

In our global warming experiments the global ocean warms above 2500 meters and cools below this level (**Figure 4a**). Cooling at depth occurs in the Northern Ocean (Fig. 4b) and it is due to the reduction of the THC, with consequent reduction of downward advective heat transport in the North Atlantic. The reduction of upwelling in the tropics (Fig. 4c) compensates for the reduction of heating so that changes in the advective heat flux for the global ocean are small (Fig. 4a).

Heating in the upper 2500 meters is due to a decrease in both upward isopycnal diffusion and GM advection and it is concentrated at high latitudes (Fig. 4b and d), in agreement with the adjoint sensitivity study of Huang *et al*. (2003b, their fig. 5). Surface heating in global warming experiments leads to less steep isopycnal slopes, which explain the decrease in GM flux. Moreover, with increasing temperature, the density field becomes more dependent on the temperature field, because of the non-linear dependence of the expansion coefficients on temperature and salinity. Hence, the angle between isopycnals and isotherms decreases, leading to a decrease of isopycnal temperature gradient and lastly of the isopycnal flux, as noted by Gregory (2000).

Surface warming leads to greater vertical temperature gradient and increased diapycnal diffusion in the tropical region (Fig. 4c). On the other hand, in dynamically active regions like the Northern and Southern Ocean the downward diapycnal flux decreases compensating the decrease of the upward isopycnal flux (Fig. 4b and d). As pointed out in Dalan *et al*. (2004, their fig. 10), the heat balance at the high latitudes has isopycnal diffusion and diapycnal diffusion acting in the same locations. Isopycnal diffusion removes heat from the deep ocean, thus tending to increase the vertical temperature gradient, while diapycnal diffusion tends to relax this gradient by pumping heat downward. A similar tendency to compensate occurs in global warming experiments: reduction of isopycnal fluxes leads to warming at depth and a relatively small vertical temperature gradient, which then leads to a decrease in the downward diapycnal diffusion.

In **Figure 5**, the heat flux anomalies for the Northern Ocean and the tropics are separated for the Atlantic and Pacific basins. It is clear that the Northern Ocean anomalous fluxes are representative of the North Atlantic (Fig. 5a and b). The area integrated diapycnal flux anomaly

in the tropical Pacific is about three times as large as in the tropical Atlantic because the area coverage of the Pacific is twice the Atlantic's, however the decreased upwelling in the tropics is greater in the tropical Atlantic than in the tropical Pacific (Fig. 5c and d).

The analysis of vertical heat fluxes in a global warming experiment is also presented by Gregory (2000). At 160 m depth the anomalous fluxes consist of: reduction of convection in the Northern Ocean, reduction of upwelling in the tropical region and reduction of upward isopycnal diffusion in the Southern Ocean. The total heat flux anomaly in the Southern Ocean and tropics are respectively 0.55 and 0.59 Wm^{-2}, more that three times the anomaly in the Northern Ocean (0.16 Wm^{-2}).

Qualitatively our results agree with Gregory (2000) in the tropics and in the Northern Ocean, allowing for the fact that in this model the role of convection is replaced by GM advection and isopycnal diffusion (Dalan *et al*., 2004). In the Southern Ocean we find that reduction of both isopycnal diffusion and GM advection are the major contributors to the increased heat flux. Quantitatively, we note that the vertical heat balance sensibly depends on depth (Fig. 4). At high latitudes, the global heat flux anomaly decreases with depth from a value of 0.5 Wm^{-2} at the surface (Fig. 4b and d). At the tropics the anomaly is roughly constant at 0.2 Wm^{-2} between the surface and 2000 m, then decreasing with depth until the bottom of the ocean (Fig. 4c). Therefore, above 400 m both Northern and Southern Oceans contribute the most to the global heat flux anomaly, while below this level the tropics present the highest anomaly.

4b. Sensitivity to Diapycnal Diffusion

Because the anomalous isopycnal and GM fluxes are the main contributors to the total anomalous heat flux (Fig. 4a), it is natural to think that, by changing isopycnal and/or thickness diffusivities, the amount of heat penetrating the ocean would change accordingly. This is not the case as Huang *et al*. (2003c) found. Employing the same configuration of the MIT-EMIC used in this study, the authors changed both isopycnal and thickness diffusivities by a factor of two. The anomalous heat flux from isopycnal diffusion and GM advection varied, although only slightly, in the same direction as the parametric change (Huang *et al*., 2003c, their fig. 11), and the total anomalous heat flux did not vary appreciably. The same does not happen when the diapycnal diffusion changes, since the total anomalous heat flux entering the ocean sensibly increases at all depths as the diapycnal diffusion increases (**Figure 6**).

In global warming simulations the anomalous fluxes behave in the same way for all simulations given varying diapycnal diffusivity (Fig. 6). The major contributions to the heat uptake by the ocean are due to the reduction of isopycnal and GM fluxes at all depths. The magnitude of the total anomaly is directly proportional to the diffusivity, implying a greater heat penetration for high diapycnal diffusivity (Fig. 6). The reason for the increase is not directly related to the increase of diffusive heat from the ocean surface, as common physical intuition might suggest. Maximum warming is localized at high latitudes of the Atlantic Basin and in the

Southern Ocean (**Figure 7**), where isopycnal diffusion and GM advection dominate, both in magnitude in the control runs (Dalan *et al*., 2004) and in tendency in global warming experiments (Fig. 6). Note that the relative small warming at 50°N in the Atlantic basin (Fig. 7) is caused by a southward shift of the Gulf Stream, as a consequence of the slowdown of the thermohaline circulation.

The connection between elevated diapycnal diffusivity and ocean heat uptake, given by isopycnal diffusion and GM advection, is found in the temperature structure of the ocean in the control run. The thickness of the thermocline is proportional to the diapycnal diffusivity, due to the larger heat diffusion from the surface of the ocean. Hence, at high latitudes the isopycnal slope increases as the thermocline deepens, followed by an increase of isopycnal and GM fluxes. In global warming simulations, the surface warming reduces the isopycnal slopes in high latitudes of the North Atlantic (**Figure 8**) leading to a decrease of upward GM and isopycnal fluxes. The magnitude of the decrease is proportional to their control values, hence to the thickness of the thermocline and lastly to the diapycnal diffusivity. We recall that in this version of the MIT-EMIC, the role of convection is inhibited by the efficient mixing caused by isopycnal diffusion and GM advection. If the maximum isopycnal slope is reduced, convection plays a significant role in the vertical heat balance at equilibrium (Dalan *et al*., 2004, figure A2) and possibly also under global warming experiments.

4c. Comparison with CMIP2

In simulations with a 1% per year increase in CO_2 concentration, performed as part of the coupled model intercomparison project (CMIP2), the increase in global mean SAT at the time of CO_2 doubling ranged from 1.32 to 2.15 K (Covey *et al*., 2000) for different models. Similarly the results for SLR due to thermal expansion of the ocean ranged from 6.5 to 14.5 cm (S. Raper, personal communication). The different model responses are associated with differences in the models' effective climate sensitivity and rate of heat uptake. Sokolov *et al*. (2003) showed that changes in the global mean SAT and SLR simulated by different AOGCMs can be reproduced by the MIT 2D climate model (Sokolov and Stone, 1998) with an appropriate choice of the 2D model's climate sensitivity and its rate of heat uptake in the ocean. The latter is simulated by diffusing heat anomalies into the deep ocean with an effective global mean diffusion coefficient, K_v, which represents the net effect of all oceanic processes. For the models used in CMIP2, K_v ranges from 4 to 25 cm^2/s (Sokolov *et al*., 2003).

In our OGCM we can vary the heat uptake by varying the diapycnal diffusion coefficient. Observationally based estimates of this coefficient range from 0.1 to 1.0 cm^2/s (Munk and Wunsch, 1998). **Table 1** shows how varying this coefficient over this range changes the response of our model. The different responses give an estimate of the uncertainty in global warming projections due to uncertainty in the diapycnal diffusion. Table 1 also gives the values of K_v in the 2D model that allow it to mimic the response of our model for different values of the

Table 1. Surface air temperature anomaly, sea level rise due to thermal expansion at the time of doubling CO_2, and effective diffusivity of the MIT 2D climate model in global warming experiments with different diapycnal diffusivity.

Diapycnal Diffusivity (cm^2/s)	0.1	0.2	0.5	1.0
Change in Surface Air Temperature (K)	1.83	1.68	1.57	1.46
Sea Level Rise (cm)	9.2	10.3	12.1	13.1
Equivalent K_v (cm^2/s)	5.0	7.5	37	125

diapycnal diffusivity. These values of K_v cover most of the range of the CMIP2 models. Thus the MIT-EMIC with varying values of the diapycnal diffusivity can also be used in sensitivity studies where the effect of different rates of oceanic heat uptake need to be taken into account (Webster *et al.*, 2003). We note that the range of values for the change in SAT and SLR shown in Table 1 are not as large as for the CMIP2 models, because the MIT-EMIC results shown in Table 1 are for a fixed climate sensitivity of 2.8 K, whereas the climate sensitivity of the CMIP2 models ranges from 1.9 K to 4.2 K.

5. CONCLUSIONS

We analyzed the sensitivity of the climate to diapycnal diffusivity for a global warming scenario focusing on the behavior of the THC and on the rate of heat uptake by the ocean. This study is the first to explore the sensitivity to diapycnal diffusion of the ocean using a coupled model with a 3D ocean component.

Increasing the carbon dioxide level in the atmosphere at a rate of 1% per year for 75 years leads to a slowdown of the THC circulation for about 100 years and recovery afterwards. The rate at which the circulation recovers and the percentage recovery at the end of the simulation vary with the diapycnal diffusion in an unpredictable fashion. For the largest (1.0 cm^2/s) and smallest (0.1 cm^2/s) values of the diapycnal diffusivity, recovery is slow and in-complete at the end of the 1000 years integration. For diapycnal diffusivity equal to 0.5 cm^2/s the circulation recovers rapidly, while for diapycnal diffusivity equal to 0.2 cm^2/s the circulation first recovers completely its control strength. For the first 60-70 years of integration, what differentiates the response of the climate system (as the diapycnal diffusion varies) is the relative contribution of temperature and salinity in determining the evolution of steric height gradient between North and South Atlantic. In climate systems with small diapycnal diffusivity, the temperature variations largely explain the changes in steric height gradient, while in highly diffusive ocean models the salinity variations are comparable to the temperature's in terms of steric height. Thus, the sensitivity of the model to surface heat and moisture flux depends on the diapycnal diffusivity. Both the strength of the THC and the thickness of the thermocline highly depend on the diapycnal diffusivity. As a consequences also the advective timescale and the magnitude of the GM advective fluxes and both isopycnal and diapycnal fluxes are related to the diapycnal diffusivity. Therefore the relation between sensitivity to surface forcing and diapycnal diffusivity is likely to be an indirect consequence of the relation between the latter parameter and the state of the climate at equilibrium.

The rate of ocean heat uptake under global warming experiments increases with diapycnal diffusivity. The increase in ocean heat content is related to the decrease in bolus velocity (GM) advection and isopycnal diffusion that are the major heat sinks. The role of convection is negligible in this version of the model since first GM advection and then isopycnal diffusion, efficiently mix the surface ocean. At high latitudes, the rise in sea surface temperature due to global warming leads to a decrease of isopycnal slope and in the temperature gradient along isopycnals. Consequently both GM advection and isopycnal diffusion are reduced inducing warming of the sub-surface ocean. At equilibrium, the magnitude of these processes is greater for a thicker thermocline, thus for larger diapycnal diffusivity. In global warming experiments the decrease in upward isopycnal diffusion and GM advection is proportional to their value at equilibrium, hence the rate of ocean heat uptake is larger for larger diapycnal diffusivity.

The uncertainty in the global value of the diapycnal diffusivity reflects on the uncertainty in ocean heat uptake under global warming scenarios, which in turn regulates the increase in Surface Air Temperature (SAT) and Sea Level Rise (SLR). Our calculations suggest that an increase of the diapycnal diffusivity by a factor 10 (from 0.1 cm^2/s to 1.0 cm^2/s) leads, at the time of doubling CO_2, to a decrease of SAT of 0.4 K and an increase of SLR due to thermal expansion of 4 cm.

6. REFERENCES

Bryan, K., 1984: Accelerating the convergence to equilibrium of ocean-climate models. *Journal of Physical Oceanography*, **14**, 666-673.

Bryan, F., 1987: Parameter Sensitivity of Primitive Equation Ocean General Circulation Models. *Journal of Physical Oceanography*, **17**, 970-985.

Covey, C., K. M. AchutaRao, S. J. Lambert, and K. E. Taylor, 2000: Intercomparison of present and future climates simulated by coupled ocean-atmosphere GCMs. PCMDI Report #66, 52 pp.

Dalan, F., P. H. Stone, I. V. Kamekovich, and J. R. Scott, 2004: Sensitivity of Climate to Diapycnal Diffusivity in the Ocean. Part I: Equilibrium State. *Journal of Climate*, Submitted.

Forest, C. E., P. H. Stone, A. P. Sokolov, M. R. Allen, and M. D. Webster, 2002: Quantifying Uncertainties in Climate System Properties with the Use of Recent Climate Observations. *Science*, **295**, 113-117.

Ganopolsky, A., V. Petoukhov, S. Rahmstorf, V. Brovkin, M. Claussen, A. Eliseev, and C. Kubatzki, 2001: CLIMBER-2: a climate system model of intermediate complexity. Part II: model sensitivity. *Climate Dynamics*, **17**, 735-751.

Gent, P. R., and J.C. McWillams, 1990: Isopycnal Mixing in Ocean Circulation Models. *Journal of Physical Oceanography*, **20**, 150-155.

Gordon, C., C. Cooper, C. A. Senior, H. Banks, J. M. Gregory, T. C. Johns, J. F. B. Mitchell, and R. A. Woods, 2000: The simulation of SST, sea ice extents and ocean heat transports in a version of the Hadley Centre coupled model without flux adjustments. *Climate Dynamics*, **16**, 147-168.

Gregory, J. M., 2000: Vertical heat transports in the ocean and their effect on time-dependent climate change. *Climate Dynamics*, **16**, 501-515.

Hansen, J., G. Russel, D. Rind, P. Stone, A. Lacis, S. Lebedeff, R. Ruedy, and L. Travis, 1983: Efficient three-dimensional global models for climate studies: Model I and II. *Monthly Weather Review*, **111**, 609-662.

Houghton, J. T., Y. Ding, D. J. Griggs, M. Noguer, P. J. van der Linden, X. Dai, K. Maskell, and C. A. Johnson, 2001: *Climate Change 2001: The Scientific Basis*. Cambridge University press, 881 pp.

Huang, B., P. H. Stone, and C. Hill, 2003a: Sensitivities of deep-ocean heat uptake and heat content to surface fluxes and subgrid-scale parameters in an ocean general circulation model with idealized geometry. *Journal of Geophysical Research*, **108**, 3015, doi: 10.1029/2001JC001218.

Huang, B., P. H. Stone, A. P. Sokolov, and I. V. Kamenkovich, 2003b: The Deep-Ocean Heat Uptake in Transient Climate Change. *Journal of Climate*, **16**, 1352-1363.

Huang, B., P. H. Stone, A. P. Sokolov, and I. V. Kamenkovich, 2003c: Ocean Heat Uptake in Transient Climate Change: Mechanisms and Uncertainty due to Subgrid-Scale Eddy Mixing. *Journal of Climate*, **16**(20): 3344-3356.

Huang, R. X., 1999: Mixing and Energetics of the Oceanic Thermohaline Circulation. *Journal of Physical Oceanography*, **29**, 727-746.

Hughes, T. C. M., and A. J. Weaver, 1994: Multiple equilibria of an asymmetric two-basin ocean model. *Journal of Physical Oceanography*, **24**, 619-637.

Jiang, S., P. H. Stone, and P. Malanotte-Rizzoli, 1999: An assessment of the Geophysical Fluid Dynamics Laboratory ocean model with coarse resolution: Annual-mean climatology. *Journal of Geophysical Research*, **104**, 25623-25645.

Johns, T. C., R. E. Carnell, J. F. Crossley, J. M. Gregory, J. F. B. Mitchell, C. A. Senior, S. F. B. Tett, and R. A. Woods, 1997: The second Hadley Centre coupled ocean-atmosphere GCM: model description, spinup and validation. *Climate Dynamics*, **13**, 103-134.

Kamenkovich, I. V., A. P. Sokolov, and P. H. Stone, 2002: An efficient climate model with a 3D ocean and a statistical-dynamical atmosphere. *Climate Dynamics*, **19**, 585-598.

Kamenkovich, I. V., A. P. Sokolov, and P. H. Stone, 2003: Feedbacks affecting the response of the thermohaline circulation to increasing CO_2: a study with a model of intermediate complexity. *Climate Dynamics*, **21**, 119-130.

Knutti, R., and T. F. Stocker, 2002: Limited Predictability of the Future Thermohaline Circulation Close to an Instability Threshold. *Journal of Climate*, **15**, 179-186.

Large, W. G., J. C. McWilliams, and S. C. Doney, 1994: Oceanic Vertical Mixing: A Review and a Model with a Nonlocal Boundary Layer Parameterization. *Reviews of Geophysics*, **32**, 363-403.

Ledwell, J. R., E. T. Montgomery, K. L. Polzin, L. C. St. Laurent, R. W. Schmitt, and J. M. Toole, 2000: Evidence for enhanced mixing over rough topography in the abyssal ocean. *Nature*, **403**, 179-182.

Manabe, S., and R. J. Stouffer, 1999: Are two modes of thermohaline circulation stable? *Tellus*, **51A**, 400-411.

Marotzke, J., 1997: Boundary Mixing and the Dynamics of Three-Dimensional Thermohaline Circulation. *Journal of Physical Oceanography*, **27**, 1713-1728.

Munk, W., and C. Wunsch, 1998: Abyssal recipes II: energetics of tidal and wind mixing. *Deep Sea Research*, **45**, 1977-2010.

Pacanowski, R. C., and S. G. H. Philander, 1981: Parameterization of Vertical Mixing in Numerical Models of Tropical Oceans. *Journal of Physical Oceanography*, **11**, 1443-1451.

Pacanowski, R. C., 1996: *MOM2 version 2.0: Documentation User's Guide and Reference Manual*. Geophysical Fluid Dynamics Laboratory, Technical Report 3.2, Princeton, New Jersey.

Park, Y. G., and K. Bryan, 2000: Comparison of Thermally Driven Circulations from a Depth-Coordinate Model and an Isopycnal-Layer Model. Part I: Scaling-Law Sensitivity to Vertical Diffusivity. *Journal of Physical Oceanography*, **30**, 590-605.

Polzin, K. L., J. M. Toole, J. R. Ledwell, and R. W. Schmitt, 1997: Spatial Variability of Turbulent Mixing in the Abyssal Ocean. *Science*, **276**, 93-96.

Prinn, R., H. Jacoby, A. Sokolov, C. Wang, X. Xiao, Z. Yang, R. Eckaus, P. Stone, D. Ellerman, J. Melillo, J. Fitzmaurice, D. Kicklighter, G. Holian, & Y. Liu. Integrated Global System Model for Climate Policy Assessment: Feedbacks and Sensitivity Studies. *Climatic Change*, **41**, 469-546.

Redi, M. H., 1982: Oceanic isopycnal mixing by coordinate rotation. *Journal of Physical Oceanography*, **12**, 1154-1158.

Sokolov, A. P., and P. H. Stone, 1998: A flexible climate model for use in integrated assessments. *Climate Dynamics*, **14**, 291-303.

Sokolov, A. P., C. E. Forest and P. H. Stone, 2003: Comparing Oceanic Heat Uptake in AOGCM Trasient Climate Change Experiments. *Journal of Climate*, **16**, 1573-1582.

Stocker, T. F., and A. Schmittner, 1997: Influence of CO_2 emissions rates on the stability of the thermohaline circulation. *Nature*, **388**, 862-865.

Stone, P. H., and M-S. Yao, 1990: Development of a Two-Dimensional Zonally Averaged Statistical-Dynamical Model. Part III: The Parameterization of the Eddy Fluxes of Heat and Moisture. *Journal of Climate*, **3**, 726-740.

Thorpe, R. B., J. M. Gregory, T. C. Johns, R. A. Woods, and J. F. B. Mitchell, 2001: Mechanisms Determining the Atlantic Thermohaline Circulation Response to Greenhouse Gas Forcing in a Non-Flux-Adjusted Coupled Climate Model. *Journal of Climate*, **14**, 3102-3116.

Tokioka, T., and A. Noda, 2001: Global Warming Projection Studies at the Meteorological Research Institute/JMA. *Present and Future of Modeling Global Environment Change: Toward Integrated Modeling*, T. Matsuno and H. Kida, Ed., TERRAPUB, 1-14.

Webster, M., C. Forest, J. Reilly, M. Babiker, D. Kicklighter, M. Mayer, R. Prinn, M. Sarofim, A. Sokolov, P. H. Stone and C. Wang, 2003: Uncertainty analysis of climate change and policy response. *Climatic Change*, **61:** 295-320.

Zhang, J., R. W. Schmitt, and R. X. Huang, 1999: The Relative Influence of Diapycnal Mixing and Hydrologic Forcing on the Stability of the Thermohaline Circulation. *Journal of Physical Oceanography*, **29**, 1096-1108.

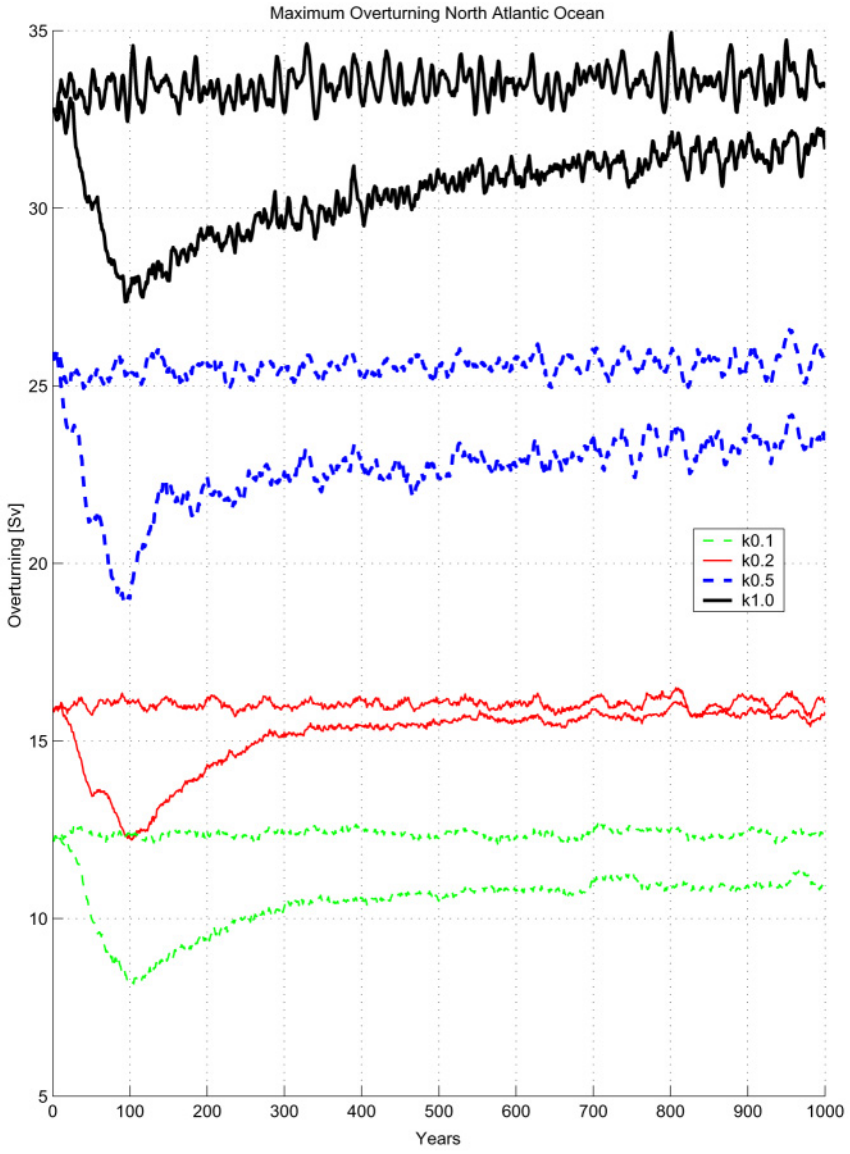

Figure 1: Maximum meridional streamfunction in the North Atlantic Ocean. For each value of the diapycnal diffusivity, both control experiment and global warming overturning strength is displayed. The control overturning strength of the THC fluctuates around a mean value that depends on the diapycnal diffusivity. In global warming experiments the THC strength diminishes for about 100 years and then partially or fully recovers its original value. Diffusivity 0.1 cm^2/s thin dashed line, 0.2 cm^2/s thin solid line, 0.5 cm^2/s thick dashed line and 1.0 cm^2/s thick solid line.

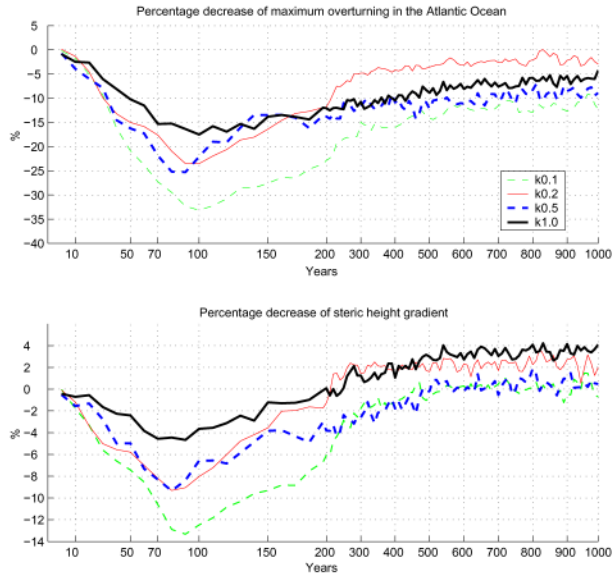

Figure 2: Percentage reduction of maximum **(top)** meridional streamfunction, and **(bottom)** steric height gradient in the Atlantic Ocean for different values of the diapycnal diffusivity: diffusivity 0.1 cm^2/s thin dashed line, 0.2 cm^2/s thin solid line, 0.5 cm^2/s thick dashed line and 1.0 cm^2/s thick solid line. Note the stretching of the horizontal axis.

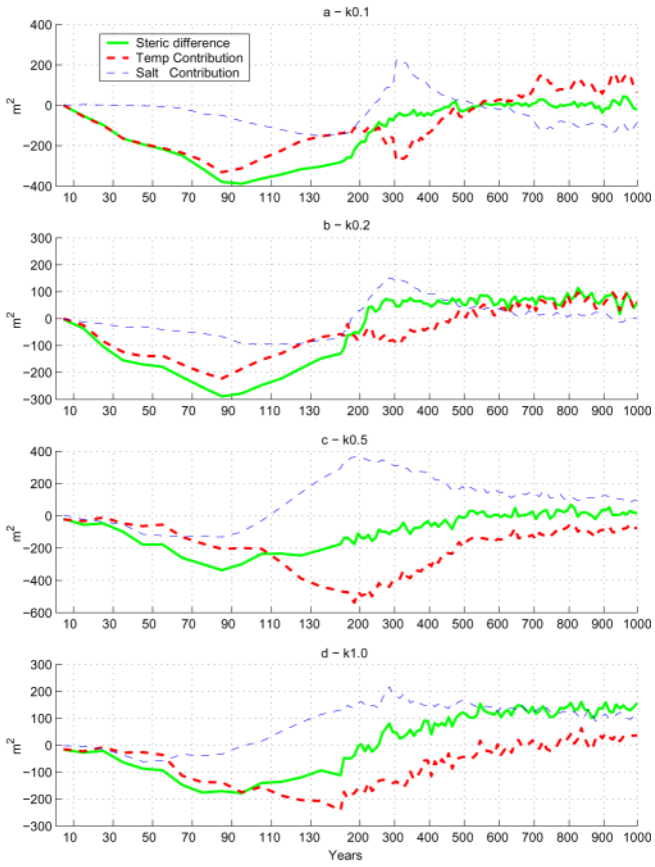

Figure 3: Steric height gradient anomaly (solid) and its temperature (thick dashed) and salinity (thin dashed) contribution in the Atlantic Ocean for different values of the diapycnal diffusivity: **(a)** 0.1 cm^2/s; **(b)** 0.2 cm^2/s; **(c)** 0.5 cm^2/s; and **(d)** 1.0 cm^2/s. Note the stretching of the horizontal axis.

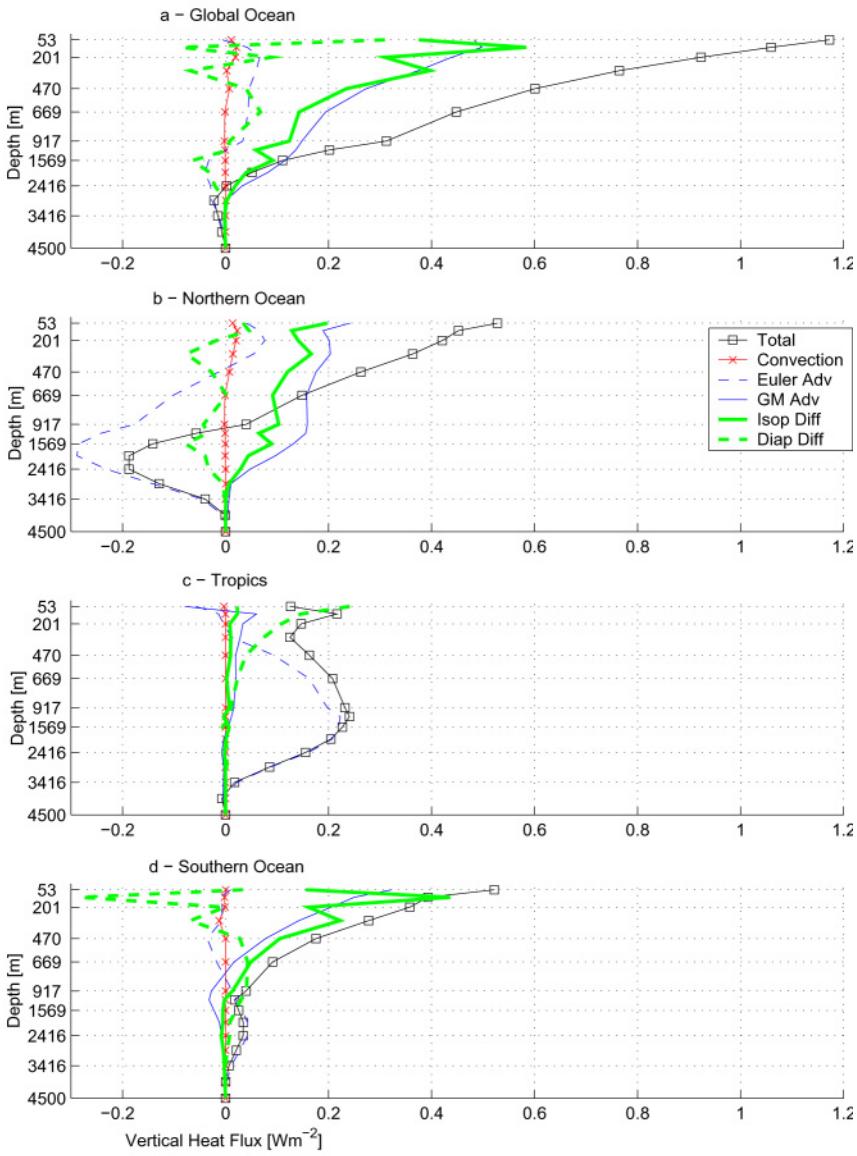

Figure 4: Global warming experiment. **(a)** Vertical heat flux anomalies for global ocean, **(b)** Northern Ocean, **(c)** Tropics, and **(d)** Southern Ocean, for diapycnal diffusivity 0.5 cm^2/s, averaged from years 66 to 75 of simulation. Positive (negative) sign indicates increase (decrease) for downward fluxes or decrease (increase) for upward fluxes with respect to equilibrium. Upward fluxes are isopycnal diffusion, GM advection and convection. Downward fluxes are advection and diapycnal diffusion.

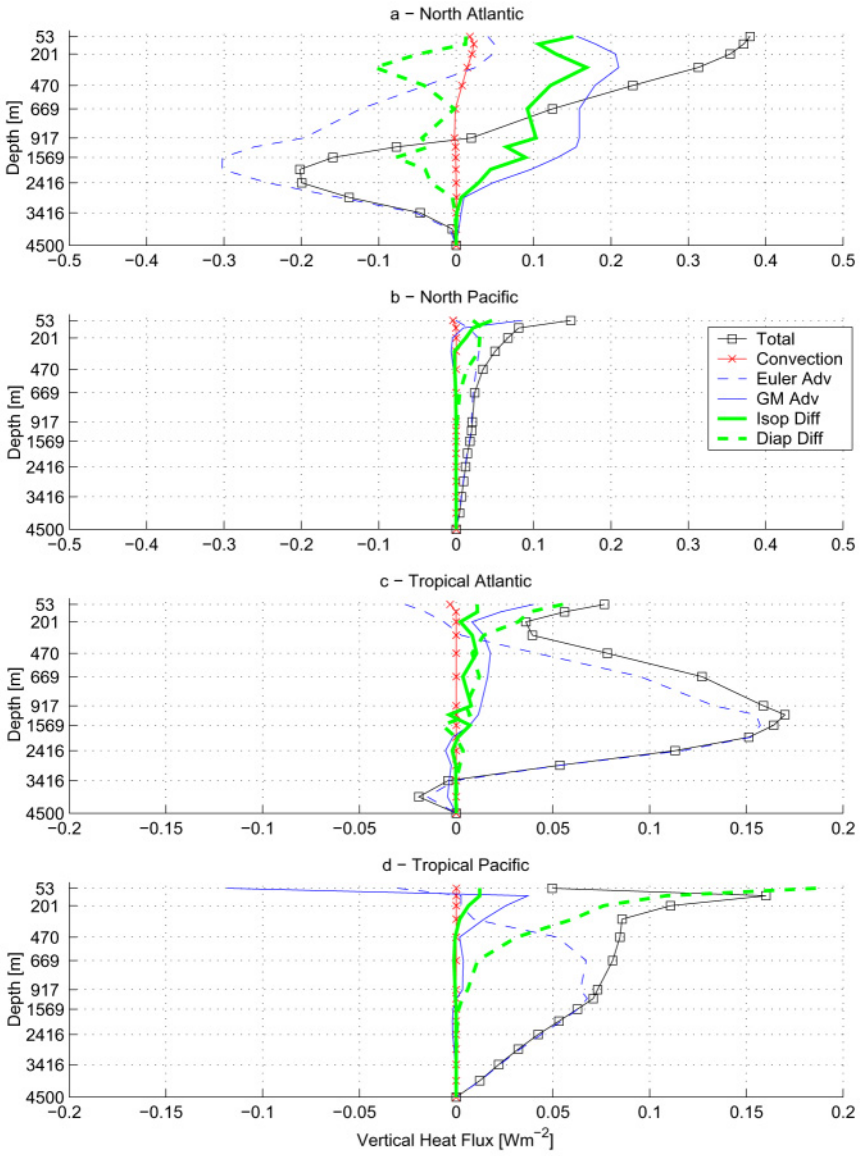

Figure 5: Global warming experiment. **(a)** Vertical heat flux anomalies for the North Atlantic, **(b)** North Pacific, **(c)** tropical Atlantic, and **(d)** tropical Pacific, for diapycnal diffusivity 0.5 cm^2/s, averaged from years 66 to 75 of simulation. Positive (negative) sign indicates increase (decrease) for downward fluxes or decrease (increase) for upward fluxes with respect to equilibrium. Upward fluxes are isopycnal diffusion, GM advection and convection. Downward fluxes are advection and diapycnal diffusion.

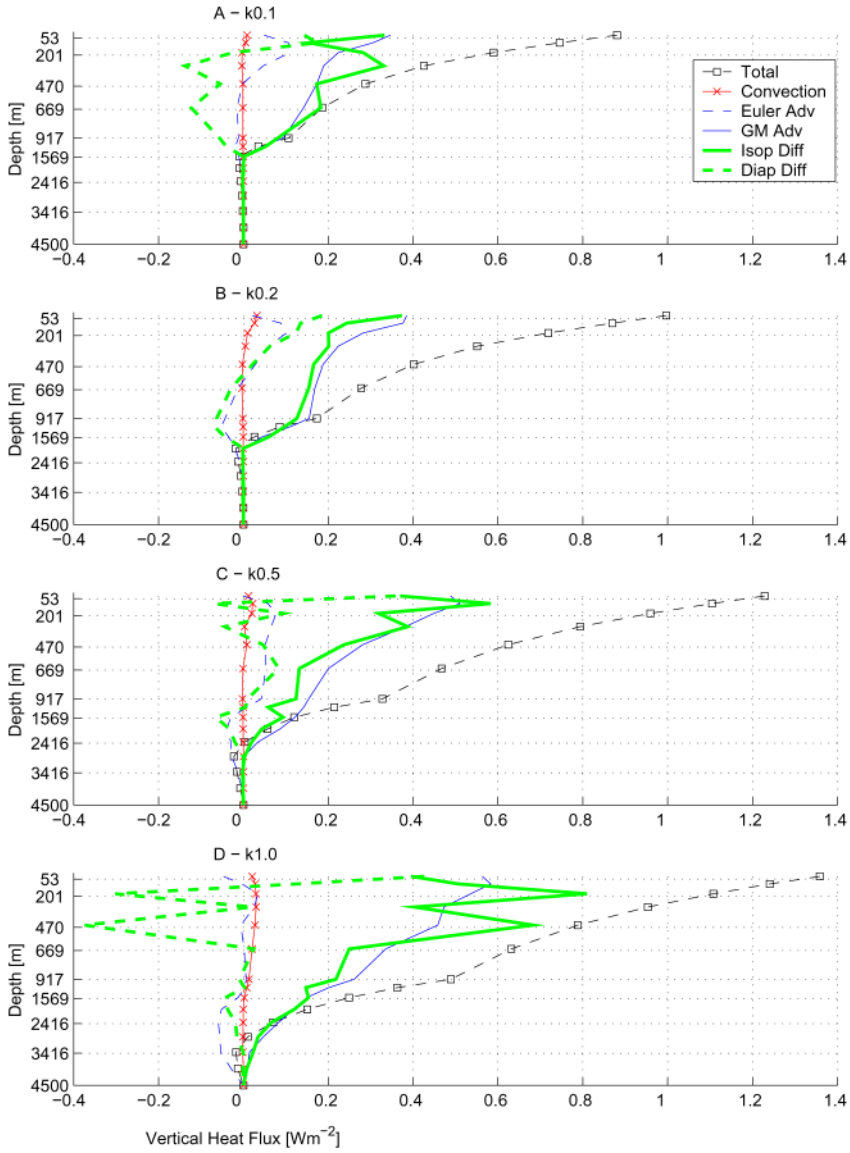

Figure 6: Changes in vertical heat fluxes due to global warming for the global ocean and for diapycnal diffusivity **(a)** 0.1 cm^2/s, **(b)** 0.2 cm^2/s, **(c)** 0.5 cm^2/s, **(d)** 1.0 cm^2/s, averaged from years 66 to 75 of simulation. Positive (negative) sign indicates increase (decrease) for downward fluxes or decrease (increase) for upward fluxes with respect to equilibrium. Upward fluxes are isopycnal diffusion, GM advection and convection. Downward fluxes are advection and diapycnal diffusion.

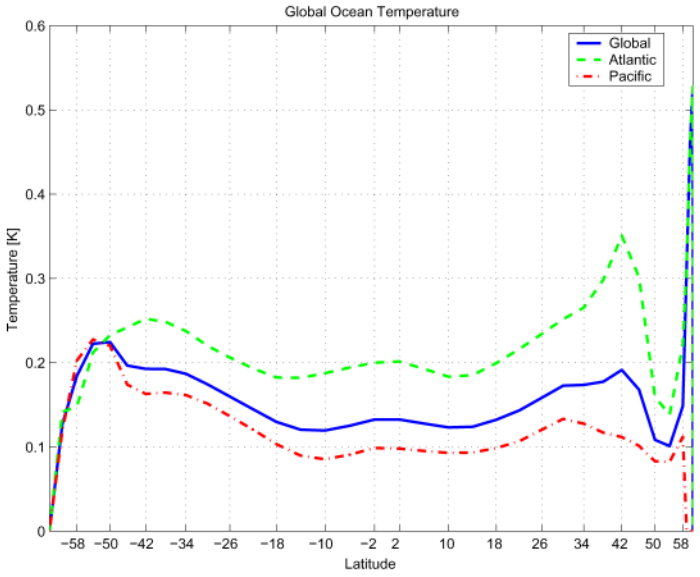

Figure 7: Meridional distribution of global ocean temperature anomaly at the time of CO_2 doubling for diapycnal diffusivity 0.5 cm^2/s.

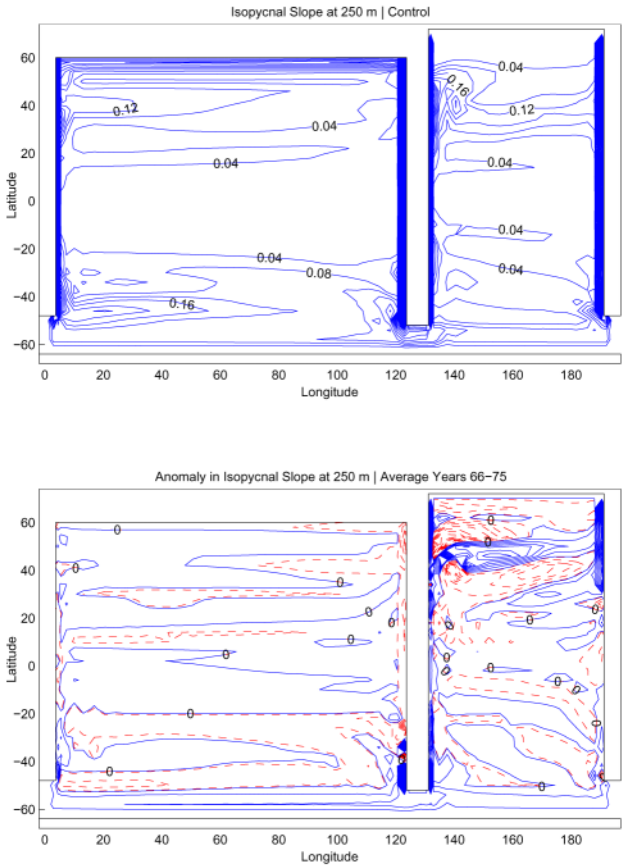

Figure 8: Modulus of the isopycnal slope **(top)** and its anomaly due to global warming **(bottom)** at 250 m depth for diapycnal diffusivity 0.5 cm^2/s. Solid line denotes positive values and dashed line denotes negative values.

REPORT SERIES of the MIT *Joint Program on the Science and Policy of Global Change*

1. **Uncertainty in Climate Change Policy Analysis** *Jacoby & Prinn* December 1994
2. **Description and Validation of the MIT Version of the GISS 2D Model** *Sokolov & Stone* June 1995
3. **Responses of Primary Production & C Storage to Changes in Climate and Atm. CO_2 Concentration** *Xiao et al.* Oct 1995
4. **Application of the Probabilistic Collocation Method for an Uncertainty Analysis** *Webster et al.* January 1996
5. **World Energy Consumption and CO_2 Emissions: 1950-2050** *Schmalensee et al.* April 1996
6. **The MIT Emission Prediction and Policy Analysis (EPPA) Model** *Yang et al.* May 1996
7. **Integrated Global System Model for Climate Policy Analysis** *Prinn et al.* June 1996 (*superseded by No. 36*)
8. **Relative Roles of Changes in CO_2 & Climate to Equilibrium Responses of NPP & Carbon Storage** *Xiao et al.* June 1996
9. **CO_2 Emissions Limits: *Economic Adjustments and the Distribution of Burdens*** *Jacoby et al.* July 1997
10. **Modeling the Emissions of N_2O & CH_4 from the Terrestrial Biosphere to the Atmosphere** *Liu* August 1996
11. **Global Warming Projections: *Sensitivity to Deep Ocean Mixing*** *Sokolov & Stone* September 1996
12. **Net Primary Production of Ecosystems in China and its Equilibrium Responses to Climate Changes** *Xiao et al.* Nov 1996
13. **Greenhouse Policy Architectures and Institutions** *Schmalensee* November 1996
14. **What Does Stabilizing Greenhouse Gas Concentrations Mean?** *Jacoby et al.* November 1996
15. **Economic Assessment of CO_2 Capture and Disposal** *Eckaus et al.* December 1996
16. **What Drives Deforestation in the Brazilian Amazon?** *Pfaff* December 1996
17. **A Flexible Climate Model For Use In Integrated Assessments** *Sokolov & Stone* March 1997
18. **Transient Climate Change & Potential Croplands of the World in the 21st Century** *Xiao et al.* May 1997
19. **Joint Implementation: *Lessons from Title IV's Voluntary Compliance Programs*** *Atkeson* June 1997
20. **Parameterization of Urban Sub-grid Scale Processes in Global Atmospheric Chemistry Models** *Calbo et al.* July 1997
21. **Needed: A Realistic Strategy for Global Warming** *Jacoby, Prinn & Schmalensee* August 1997
22. **Same Science, Differing Policies; *The Saga of Global Climate Change*** *Skolnikoff* August 1997
23. **Uncertainty in the Oceanic Heat and Carbon Uptake & their Impact on Climate Projections** *Sokolov et al.* Sept 1997
24. **A Global Interactive Chemistry and Climate Model** *Wang, Prinn & Sokolov* September 1997
25. **Interactions Among Emissions, Atmospheric Chemistry and Climate Change** *Wang & Prinn* September 1997
26. **Necessary Conditions for Stabilization Agreements** *Yang & Jacoby* October 1997
27. **Annex I Differentiation Proposals: *Implications for Welfare, Equity and Policy*** *Reiner & Jacoby* October 1997
28. **Transient Climate Change & Net Ecosystem Production of the Terrestrial Biosphere** *Xiao et al.* November 1997
29. **Analysis of CO_2 Emissions from Fossil Fuel in Korea: 1961–1994** *Choi* November 1997
30. **Uncertainty in Future Carbon Emissions: *A Preliminary Exploration*** *Webster* November 1997
31. **Beyond Emissions Paths: *Rethinking the Climate Impacts of Emissions Protocols*** *Webster & Reiner* November 1997
32. **Kyoto's Unfinished Business** *Jacoby, Prinn & Schmalensee* June 1998
33. **Economic Development and the Structure of the Demand for Commercial Energy** *Judson et al.* April 1998
34. **Combined Effects of Anthropogenic Emissions & Resultant Climatic Changes on Atmosph. OH** *Wang & Prinn* April 1998
35. **Impact of Emissions, Chemistry, and Climate on Atmospheric Carbon Monoxide** *Wang & Prinn* April 1998
36. **Integrated Global System Model for Climate Policy Assessment: *Feedbacks and Sensitivity Studies*** *Prinn et al.* June 1998
37. **Quantifying the Uncertainty in Climate Predictions** *Webster & Sokolov* July 1998
38. **Sequential Climate Decisions Under Uncertainty: *An Integrated Framework*** *Valverde et al.* September 1998
39. **Uncertainty in Atmospheric CO_2 (Ocean Carbon Cycle Model Analysis)** *Holian* October 1998 (*superseded by No. 80*)
40. **Analysis of Post-Kyoto CO_2 Emissions Trading Using Marginal Abatement Curves** *Ellerman & Decaux* October 1998
41. **The Effects on Developing Countries of the Kyoto Protocol & CO_2 Emissions Trading** *Ellerman et al.* November 1998
42. **Obstacles to Global CO_2 Trading: *A Familiar Problem*** *Ellerman* November 1998
43. **The Uses and Misuses of Technology Development as a Component of Climate Policy** *Jacoby* November 1998
44. **Primary Aluminum Production: *Climate Policy, Emissions and Costs*** *Harnisch et al.* December 1998
45. **Multi-Gas Assessment of the Kyoto Protocol** *Reilly et al.* January 1999
46. **From Science to Policy: *The Science-Related Politics of Climate Change Policy in the U.S.*** *Skolnikoff* January 1999
47. **Constraining Uncertainties in Climate Models Using Climate Change Detection Techniques** *Forest et al.* April 1999
48. **Adjusting to Policy Expectations in Climate Change Modeling** *Shackley et al.* May 1999
49. **Toward a Useful Architecture for Climate Change Negotiations** *Jacoby et al.* May 1999
50. **A Study of the Effects of Natural Fertility, Weather & Productive Inputs in Chinese Agriculture** *Eckaus & Tso* July 1999
51. **Japanese Nuclear Power and the Kyoto Agreement** *Babiker, Reilly & Ellerman* August 1999
52. **Interactive Chemistry and Climate Models in Global Change Studies** *Wang & Prinn* September 1999
53. **Developing Country Effects of Kyoto-Type Emissions Restrictions** *Babiker & Jacoby* October 1999
54. **Model Estimates of the Mass Balance of the Greenland and Antarctic Ice Sheets** *Bugnion* October 1999
55. **Changes in Sea-Level Associated with Modifications of Ice Sheets over 21st Century** *Bugnion* October 1999
56. **The Kyoto Protocol and Developing Countries** *Babiker, Reilly & Jacoby* October 1999
57. **Can EPA Regulate GHGs Before the Senate Ratifies the Kyoto Protocol?** *Bugnion & Reiner* November 1999
58. **Multiple Gas Control Under the Kyoto Agreement** *Reilly, Mayer & Harnisch* March 2000

Contact the Joint Program Office to request a copy. The Report Series is distributed at no charge.

REPORT SERIES of the MIT *Joint Program on the Science and Policy of Global Change*

59. **Supplementarity: *An Invitation for Monopsony?*** *Ellerman & Sue Wing* April 2000
60. **A Coupled Atmosphere-Ocean Model of Intermediate Complexity** *Kamenkovich et al.* May 2000
61. **Effects of Differentiating Climate Policy by Sector: *A U.S. Example*** *Babiker et al.* May 2000
62. **Constraining Climate Model Properties Using Optimal Fingerprint Detection Methods** *Forest et al.* May 2000
63. **Linking Local Air Pollution to Global Chemistry and Climate** *Mayer et al.* June 2000
64. **The Effects of Changing Consumption Patterns on the Costs of Emission Restrictions** *Lahiri et al.* August 2000
65. **Rethinking the Kyoto Emissions Targets** *Babiker & Eckaus* August 2000
66. **Fair Trade and Harmonization of Climate Change Policies in Europe** *Viguier* September 2000
67. **The Curious Role of "Learning" in Climate Policy: *Should We Wait for More Data?*** *Webster* October 2000
68. **How to Think About Human Influence on Climate** *Forest, Stone & Jacoby* October 2000
69. **Tradable Permits for GHG Emissions: *A primer with reference to Europe*** *Ellerman* November 2000
70. **Carbon Emissions and The Kyoto Commitment in the European Union** *Viguier et al.* February 2001
71. **The MIT Emissions Prediction and Policy Analysis Model: *Revisions, Sensitivities and Results*** *Babiker et al.* Feb 2001
72. **Cap and Trade Policies in the Presence of Monopoly and Distortionary Taxation** *Fullerton & Metcalf* March 2001
73. **Uncertainty Analysis of Global Climate Change Projections** *Webster et al.* March 2001 (*superseded by No. 95*)
74. **The Welfare Costs of Hybrid Carbon Policies in the European Union** *Babiker et al.* June 2001
75. **Feedbacks Affecting the Response of the Thermohaline Circulation to Increasing CO_2** *Kamenkovich et al.* July 2001
76. **CO_2 Abatement by Multi-fueled Electric Utilities: *An Analysis Based on Japanese Data*** *Ellerman & Tsukada* July 2001
77. **Comparing Greenhouse Gases** *Reilly, Babiker & Mayer* July 2001
78. **Quantifying Uncertainties in Climate System Properties using Recent Climate Observations** *Forest et al.* July 2001
79. **Uncertainty in Emissions Projections for Climate Models** *Webster et al.* August 2001
80. **Uncertainty in Atmospheric CO_2 Predictions from a Global Ocean Carbon Cycle Model** *Holian et al.* Sep 2001
81. **A Comparison of the Behavior of AO GCMs in Transient Climate Change Experiments** *Sokolov et al.* December 2001
82. **The Evolution of a Climate Regime: *Kyoto to Marrakech*** *Babiker, Jacoby & Reiner* February 2002
83. **The "Safety Valve" and Climate Policy** *Jacoby & Ellerman* February 2002
84. **A Modeling Study on the Climate Impacts of Black Carbon Aerosols** *Wang* March 2002
85. **Tax Distortions and Global Climate Policy** *Babiker, Metcalf & Reilly* May 2002
86. **Incentive-based Approaches for Mitigating GHG Emissions: *Issues and Prospects for India*** *Gupta* June 2002
87. **Sensitivities of Deep-Ocean Heat Uptake and Heat Content to Surface Fluxes and Subgrid-Scale Parameters in an Ocean GCM with Idealized Geometry** *Huang, Stone & Hill* September 2002
88. **The Deep-Ocean Heat Uptake in Transient Climate Change** *Huang et al.* September 2002
89. **Representing Energy Technologies in Top-down Economic Models using Bottom-up Info** *McFarland et al.* Oct 2002
90. **Ozone Effects on NPP and C Sequestration in the U.S. Using a Biogeochemistry Model** *Felzer et al.* November 2002
91. **Exclusionary Manipulation of Carbon Permit Markets: *A Laboratory Test*** *Carlén* November 2002
92. **An Issue of Permanence: *Assessing the Effectiveness of Temporary Carbon Storage*** *Herzog et al.* December 2002
93. **Is International Emissions Trading Always Beneficial?** *Babiker et al.* December 2002
94. **Modeling Non-CO_2 Greenhouse Gas Abatement** *Hyman et al.* December 2002
95. **Uncertainty Analysis of Climate Change and Policy Response** *Webster et al.* December 2002
96. **Market Power in International Carbon Emissions Trading: *A Laboratory Test*** *Carlén* January 2003
97. **Emissions Trading to Reduce GHG Emissions in the US: *The McCain-Lieberman Proposal*** *Paltsev et al.* June 2003
98. **Russia's Role in the Kyoto Protocol** *Bernard et al.* June 2003
99. **Thermohaline Circulation Stability: *A Box Model Study*** *Lucarini & Stone* June 2003
100. **Absolute vs. Intensity-Based Emissions Caps** *Ellerman & Sue Wing* July 2003
101. **Technology Detail in a Multi-Sector CGE Model: *Transport Under Climate Policy*** *Schafer & Jacoby* July 2003
102. **Induced Technical Change and the Cost of Climate Policy** *Sue Wing* September 2003
103. **Past and Future Effects of Ozone on Net Primary Production and Carbon Sequestration Using a Global Biogeochemical Model** *Felzer et al.* October 2003 [Revised January 2004]
104. **A Process-Based Modeling Analysis of Methane Exchanges Between Alaskan Terrestrial Ecosystems and the Atmosphere** *Zhuang et al.* November 2003
105. **Analysis of Strategies of Companies under Carbon Constraint: *Relationship Between Profit Structure and Carbon/Fuel Price Uncertainty*** *Hashimoto* January 2004
106. **Climate Prediction: *The Limits of Ocean Models*** *Stone* February 2004
107. **Informing Climate Policy Given Incommensurable Benefits Estimates** *Jacoby* February 2004
108. **Methane Fluxes Between Terrestrial Ecosystems and the Atmosphere at Northern High Latitudes During the Past Century: *A Retrospective Analysis with a Process-Based Biogeochemistry Model*** *Zhuang et al.* March 2004
109. **Sensitivity of Climate to Diapycnal Diffusivity in the Ocean: *Equilibrium State; Global Warming Scenario*** *Dalan et al.* May 2004

Contact the Joint Program Office to request a copy. The Report Series is distributed at no charge.